Article

Title:

COMPOSITUM 1 (COM1) contributes to the architectural simplification of barley inflorescence via cell wall-mediated and meristem identity signals

Authors:

N. Poursarebani[1], C. Trautewig[1], M. Melzer[1], T. Nussbaumer[3,4], U. Lundqvist[5], T. Rutten[1], T. Schmutzer[1,2], R. Brandt[1], A. Himmelbach[1], L. Altschmied[1], R. Koppolu[1], H. M. Youssef[1,2,6], M. Dalmais[7], A. Bendahmane[7], N. Stein[1], Z. Xin[8], T. Schnurbusch[1,2]

Affiliations:

[1] Leibniz Institute of Plant Genetics and Crop Plant Research (IPK), Corrensstr. 3 OT Gatersleben, D-06466 Seeland, Germany

[2] Martin Luther University Halle-Wittenberg, Faculty of Natural Sciences III, Institute of Agricultural and Nutritional Sciences, 06120 Halle, Germany

[3] Technical University of Munich and Helmholtz Center Munich, Institute of Environmental Medicine, UNIKA-T, Neusäßer Str. 47, 86156 Augsburg, Germany

[4] Helmholtz Zentrum München (HMGU), German Research Center for Environmental Health, Institute of Network Biology (INET), 85764 Neuherberg, Germany

[5] Nordic Genetic Resource Center (NordGen), Smedjevägen 3, Box P.O. 41, SE-230 53 Alnarp, Sweden

[6] Faculty of Agriculture, Cairo University, Giza, Egypt

[7] INRAE, CNRS, Institute of Plant Sciences Paris-Saclay IPS2, Univ Paris Sud, Univ Evry, Univ Paris-Diderot, Sorbonne Paris-Cite, Universite Paris-Saclay, 91405 Orsay, France

[8] USDA-ARS, Plant Stress and Germplasm Development Unit, Cropping Systems Research Laboratory, Lubbock, TX 79415, USA

*Corresponding authors. Email: Poursarebani@ipk-gatersleben.de (NP); Schnurbusch@ipk-gatersleben.de (TS)

Abstract:

Grasses have varying inflorescence shapes; however, little is known about the genetic mechanisms specifying such shapes among tribes. We identified the grass-specific TCP transcription factor COMPOSITUM 1 (COM1) expressed in inflorescence meristematic boundaries of different grasses. COM1 specifies branch-inhibition in *Triticeae* (barley) versus branch-formation in non-*Triticeae* grasses. Analyses of cell size, cell walls and transcripts revealed barley COM1 regulates cell growth, affecting cell wall properties and signaling specifically in meristematic boundaries to establish identity of adjacent meristems. *COM1* acts upstream of the boundary gene *Liguleless1* and confers meristem identity independent of the *COM2* pathway. Furthermore, COM1 is subject to purifying natural selection, thereby contributing to specification of the spike inflorescence shape. This meristem identity module has conceptual implications for both inflorescence evolution and molecular breeding in *Triticeae*.

62 **Main Text:**

63

64 The grass family (Poaceae), one of the largest angiosperm families, has evolved a striking diversity
65 of inflorescence morphologies bearing complex structures such as branches and specialized
66 spikelets [1]. These structural features are key for sorting the grass family into tribes [1]. Current grass
67 inflorescences are proposed to originate from a primitive ancestral shape exhibiting "a relatively
68 small panicle-like branching system made up of primary and secondary paracladia (branches), each
69 one standing single at the nodes" [2] (**Fig. 1A**). This ancestral panicle-like inflorescence is also
70 known as a compound spike [3-5]. Several independent or combined diversification processes
71 throughout the evolutionary history of the grass family have resulted in the broad diversity of
72 today's grass inflorescences [2,3,6]. Some tribes, e.g. *Oryzeae* (rice) and *Andropogoneae* (maize and
73 sorghum), still display ancestral and complex compound shapes, keeping true-lateral long primary
74 and secondary branches. Other grasses, such as *Brachypodium distachyon*, show lower
75 inflorescence complexity with branch length and number reduced to lateral, small pedicels ending
76 in only one multi-floretted spikelet (**Fig. 1A–C**). Inflorescences within the tribe *Triticeae*, e.g.
77 barley (*Hordeum vulgare* L.), probably evolved from the ancestral compound spike into the typical
78 unbranched spike (**Fig. 1D)**. The spike displays the least-complex inflorescence shape due to the
79 sessile nature of spikelets and reduction in rachis internodes [2,7]. Architectural variation is often
80 manifested through subtle modifications of transcriptional programs during critical transitional
81 windows of inflorescence meristem (IM) maturation [7,8] or functional divergence of key
82 transcriptional regulators and/or other genes [9,10]. Identification of key genetic determinants is
83 crucial for better understanding and explaining both the origin of grass inflorescence diversity and
84 grass developmental gene evolution. Inflorescence developmental patterning controls pollination,

grain set and grain number, and is thus highly relevant to agronomy as a target of natural and human selection.

Results

Atypical for *Triticeae*—barley *com1.a* mutant forms a branched inflorescence

To provide insight into the inflorescence architecture of *Triticeae*, we conducted a detailed phenotypic inspection of an induced barley mutant displaying non-canonical, i.e. branched, spike morphology. Barley (and other *Triticeae*) wild-type (Wt) unbranched spikes are typically composed of sessile, single-flowered spikelets arranged in a regular distichous fashion of two opposite rows directly attached to the main axis (**Fig. 1E**). The Compositum-Barley *com1.a* (*compositum 1.a*) is an induced mutant with a branched spike introgressed into the two-rowed *cv.* Bowman (BW) (**Supplementary Fig. 1**). The BW near isogenic line (NIL) of the *com1.a* allele, BW-NIL(*com1.a*), is a backcross (BC6)-derived EMS/neutron-induced mutant from *cv*. Foma [11]. The inflorescence in this mutant develops a ramified or branched architecture, resembling an ancestral compound spike (**Fig. 1E–I**), but lacks an organ called pulvinus. The pulvinus is present at the axil of lateral long branches in panicles and compound spikes of non-*Triticeae* grass species, defining branch angle extent. We observed differences in spike shape between BW and *com1.a* during early spike differentiation at the triple mound (TM) to early glume primordium (GP; in which the mutant central spikelet meristem (SM) is elongated; **Fig. 1J**) stage, becoming more apparent during later reproductive stages of late glume primordium onwards (**Fig. 1K–N**). At GP, predominantly in the basal part of the spike, meristems of the central spikelet positions undergo apparent floral reversion, displaying branch- or IM-like meristems (**Fig. 1N**). Instead of generating florets, the meristem potentially grows indefinitely and functions as an indeterminate spikelet multimer in the form of a primary branch-like structure (**Fig. 1M–N**). Such branch-like structures

109 occasionally replace other spikelet-related organs, such as the rachilla primordium (RP, the spikelet
110 axis) or glumes (**Fig. 1M–N**). The *com1* branching phenotype resembles that of the previously
111 described *compositum 2* mutant, *com2*, in which formation of branch-like structures results from
112 lack of SM identity (in Supplementary Fig. 4 of [12].
113
114 ***COM1* restricts palea cell size by thickening their cell walls**
115 Besides the branch phenotype, *com1.a* exhibits a deviation in adaxial palea morphology, having a
116 flat plane (**Fig. 1O**) versus the conventional distinct infolding observed in BW (**Fig. 1P),** *cv*. Foma,
117 and wild barley (*H. vulgare* subsp. *spontaneum*). This deviation was visible in all paleae
118 independent of their position along the spike. Histological analyses using cross sections of paleae
119 middle-areas (**Fig. 1O**) revealed distinct features of *com1.a* in which sclerenchymtous cells, in
120 particular, were expanded in size and numbers (**Fig. 1Q–R**). Cell expansion is thought to be tightly
121 linked to cell wall extensibility [13,14]. We used transmission electron microscopy (TEM) to verify
122 whether *com1.a* palea cells had altered cell wall features. Notably, mutant palea cells had clearly
123 thinner cell wall structures, thus fewer mechanical obstructions for cell expansion, indicating that
124 COM1 functions as a regulator of cell growth via cell wall modifications (**Fig. 1S–Z and**
125 **Supplementary Fig. 2**). Moreover, mutant paleae generally formed three vascular bundles (VB)
126 (**Fig. 1Q**) compared with two VBs in BW (**Fig. 1R**). By analogy to changes in palea cell walls,
127 such alterations might also explain the rescission of SM identity, providing that COM1 similarly
128 affects cell wall integrity in meristematic cells, e.g. SM cells or boundary cells (cells separating IM
129 from SMs) (see below).
130
131 ***COM1* encodes a TCP transcription factor that inhibits inflorescence branching independent**
132 **of *COM2***

To investigate the genetic basis of the *com1.a* phenotype, we constructed a genetic map by screening ~6,000 gametes for recombination events in an F_2 population (Bowman × *com1.a*) followed by further analysis of F_3 families (**Supplementary Fig. 1C–F, Supplementary Table 1, 2 and 3**) (**Supplementary Note**). This delimited a ~1.4 Mb interval carrying eight genes, one of which is a predicted transcription factor (HORVU 5Hr1G061270) entirely absent in *com1.a*, likely due to an induced deletion (**Fig. 2A**). The remaining seven genes either were not expressed or not differentially regulated between Wt and *com1.a* mutant (see below, the transcriptome analysis) (Fig1. A). To validate our candidate gene, we sequenced it in a barley TILLING population and in a set of 20 induced barley spike-branching mutants. We identified five branched mutants (*Mut.3906*, *int-h.42*, *int-h.43*, *int-h.44* and *com1.j*) missing the same transcription factor as *com1.a* (**Supplementary Fig. 3, Supplementary Table 1 and 4**) and six TILLING mutants with non-synonymous amino acid substitutions (**Fig. 2B; Supplementary Figs. 4–5; Supplementary Table 4**). *Mut.3906* was used for confirming allelism with *com1.a* (**Supplementary Note**). Together, these data confirmed unambiguously that the transcriptional regulator was responsible for the spike-branching phenotype in *com1.a*. Annotation analysis of the COM1 protein showed that it belongs to the plant-specific TCP (Teosinte branched1 (TB1)/Cycloidea/Proliferating Cell Factor) transcription factor family; COM1 contains 273 amino acids and features one basic helix-loop-helix TCP domain (**Fig. 2B**). Proteins of the TCP family fall into two classes, with COM1 belonging to class II, subclass CYC/TB1 [15,16].

We detected a higher phenotypic penetrance for spike-branching in *com1.a* (96.3%) compared to *com2.g* (78%). Double mutant (DM) plants outperformed either single mutant in grain number per spike, and supernumerary spikelet and branch production. Moreover, DM plants showed additional floral reversion in lateral spikelet positions (**Supplementary Fig. 6; Supplementary Note**), further indicating that the two loci act independently/additively in branch inhibition in barley.

Barley COM1 function evolved under purifying natural selection and affects boundary signaling

We next asked whether COM1 has experienced functional conservation or divergence within the grasses and whether its sequence composition supports possible functional alteration. We used the comprehensive phylogenetic analyses available for grass TCPs [16] and the references therein) as a starting point for our own COM1-specific phylogenic analyses. We identified first-and second-best (closest) homologs (FBH and SBH) of COM1 from sequenced grass genomes, including rice, maize, sorghum, hexaploid wheat and *Brachypodium distachyon*, as well as *Arabidopsis thaliana* (**Fig. 2C**). The homolog of maize TB1, obtained from the aforementioned grasses, was added as an out-group to the phylogeny. Our phylogenetic analysis confirmed that COM1 is restricted to grasses (**Fig. 2C**) [17-19]. The FBHs of COM1 in maize and rice were reported previously as *ZmBAD1/WAB1* and *OsREP1/DBOP* (60.3% and 65.5% sequence similarity to COM1), respectively [17-20]. Except for maize, none of the COM1 FBHs showed a duplicated copy (no in-paralogs resulting from within-genome duplication after a speciation, [21] (**Supplementary Fig. 7A–B**)). Instead, COM1 seems to be an out-paralog [21] of SBHs including the sorghum gene *SbMSD1* (44.1% sequence similarity to COM1) [22]. Functional characterization of COM1 homologs is only available for maize and rice (Table 1) [17-19].

Maize *BAD1/WAB1* transcripts are mainly detected at the IM-to-BM (branch meristem) boundary region as well as between pulvinus and lateral branches (in Fig. 3J of [18]). Consequently, loss-of-function *bad1/wab1* mutants display organ fusion (a known boundary formation defect) resulting in reduced branch number (from 5.8 in Wt to 1.3 in mutant siblings) and angle size, and more upright tassel branches [17,18]. This gene was dubbed a boundary formation gene promoting lateral meristem (e.g. branch) and axillary organ (e.g. pulvinus) formation in Wt maize [17,18].

Our TILLING analysis for the *BAD1/WAB1* ortholog in sorghum revealed one mutant (ARS180 line; A144T) with both upright tassel branches (10.95° in Wt vs. 5.2° in mutant, $P \leq 0.001$; **Fig. 3, Supplementary Table 5**) and reduced primary branch number per node (5.4 in Wt vs. 4.2 in mutant, $P \leq 0.05$; **Supplementary Table 5**). These data suggest a similar positive role of sorghum *BAD1/WAB1* in pulvinus development and branch initiation/formation, revealing functional conservation of the protein between sorghum and maize. Moreover, we detected no obvious change in sorghum palea morphology except one additional vascular bundle, similar to maize (**Table 1**). The rice homolog of *COM1*, *OsREP1/DBOP*, shows a major effect in promoting palea identity, growth and development, with no effect on branch angle or branch initiation [19,20]. Loss-of-function mutants display smaller paleae due to less differentiation and severely reduced size of palea cells; a clear contrast to palea defects in barley (**Table 1**). Our TILLING analysis of COM1 homologs in *Brachypodium distachyon* (*Bd*) identified several mutants. Phenotypic investigation of two lines (5446: Q116* and 8373: S146N) (**Supplementary Table 4, Supplementary Note**) revealed similar phenotypes to the aforementioned non-*Triticeae* species (**Table 1**) (**Fig. 3F–P**). Similarly, we observed a palea defect (**Fig. 3G**) but histological analyses revealed no changes in cell expansion, except the formation of one additional vascular bundle in each mutant (**Fig. 3L–M**). We also observed a reduction in branch angle because of smaller or absent pulvini; however, the number of lateral branches was not altered in either *Brachypodium* mutants (**Fig. 3O–Q**). In conclusion, COM1 homologs within non-*Triticeae* grasses primarily promote boundary formation and cell differentiation (as in rice palea)/proliferation (as seen for pulvinus) (**Table 1**) but also contribute to formation of lateral axillary organs, e.g. branch or pulvinus, creating more complex inflorescence structures.

To better understand the contrasting COM1 function of branch-inhibition in barley versus branch-formation in non-*Triticeae* grasses, we analyzed barley *COM1* expression using qRT-PCR and

204 semi-qPCR (Fig. 4A-C) followed by mRNA *in-situ* hybridization (**Fig. 4D-G**). Barley *COM1*
205 transcripts were detected in paleae (**Fig. 4C, F-G**), VB of the rachis (Fig. 4E), and importantly at
206 the base of forming SMs throughout the boundary region separating SMs from IM (IM-to-SM
207 boundary) and between lateral and central SMs (**Fig. 4E-F**), similar to non-*Triticeae* grass species,
208 e.g. maize. This expression pattern suggests involvement of barley *COM1* in specification of the
209 spikelet meristematic boundary. However, since central and lateral spikelets do not fuse into each
210 other or to the IM (as long branches do in maize or sorghum), barley COM1 may not be involved
211 in boundary formation *per se*. In combination with our cell wall analysis in palea cells, this implies
212 that barley COM1 may be involved in formation of meristem identity signals released from the
213 boundary region through thickened cell walls encompassing boundary cells; thus, COM1 affects
214 boundary signaling via cell wall modifications [23]. Recently acquired protein motifs specific to
215 *Triticeae* COM1 may support this functional modification (**Fig. 2D** Motifs 7, 13, 15 and 17 **and**
216 **Supplementary Fig. 8**).
217 We checked whether natural selection has acted upon barley COM1 sequence composition and
218 function, and consequently formation of unbranched spikes in barley. Re-sequencing of the barley
219 *COM1* coding sequence in a panel of 146 diverse barley landraces and 90 wild barleys [24,25]
220 (**Supplementary Table 6**) revealed very little natural sequence variation (site diversity of pi =
221 0.0006). Eleven SNPs resulted in a simple 12-haplotype network (**Supplementary Fig. 9**)
222 comprising only two main haplotypes, neither of the 12 showed mutant spike or palea phenotypes
223 (**Supplementary Fig. 9**). This suggests that barley COM1 underwent purifying natural selection
224 most likely for maintaining inflorescence shape.
225
226 **Putative transcriptional regulation for barley spike**

To further examine the molecular basis of COM1 branch inhibition within the barley spike, we performed qRT-PCR to locate *COM1* relative to other previously known spike architecture genes (**Fig. 5A**, black arrows). We localized *COM1* downstream of *VRS4 (HvRA2*; orthologous to maize *RAMOSA2*), the main regulator of row type and branch inhibition [7,12] (**Supplementary Fig. 10**). *COM2* transcript levels in immature spikes of *com1.a* were slightly lower only during later stages of development (**Supplementary Fig. 10F**).

We performed comparative RNA-seq using mRNAs from immature spikes of BW and *com1.a* as well as the mutant progenitor, *cv*. Foma, when spike patterning begins to differ between genotypes, plus two subsequent stages (**Figs. 1 and 5B; Online Materials**). Differentially expressed (DE) genes were identified in comparisons of *com1.a* versus BW and mutant versus *cv*. Foma. We found 83 genes (Log2 FoldChanges; LFC $| \geq 0.5$; adjusted $P < 0.05$) DE in at least one stage in both comparisons (**Fig. 5; Supplementary Figs. 11–12; Supplementary Source Data 1**): 18 and 65 genes up- and downregulated in BW-NIL(*com1.a*), respectively.

Among significantly downregulated genes across all three stages (**Fig. 5B**), we detected one *SQUAMOSA PROMOTER-BINDING-LIKE 8* gene (*SPL8*, HORVU2Hr1G111620) homologous to the boundary gene *LIGULELESS 1* in maize (*LG1*; *ZmSPL4*), rice *OsLG1* (*OsSPL8*) and hexaploid wheat *TaLG1* (*TaSPL8*) [26]. Similar to the known maize module (*RA2*→*WAB1*/*BAD1*→*LG1*; [17,18], we found that *VRS4*/*HvRA2*→*COM1*→*HvLG1* regulation appears to be maintained in barley. Transcriptome analysis of leaf tissues in a wheat *liguleless1* mutant revealed *TaSPL8* as a cell wall-related gene [26]. Notably, no spike-branching phenotype was reported for this erected-leaf *liguleless* mutant, most likely due to genetic redundancy.

Among other significantly downregulated genes in *com1.a*, we found important genes associated with cell wall properties and integrity (**Fig. 5D**). These include HORVU5Hr1G006430, a leucine-rich repeat receptor kinase (LRR-RLK), and HORVU3Hr1G030260 belonging to the cytochrome

P450 superfamily. LRR-RLKs and CYP450s are involved in lignin deposition to cell walls upon cellulose biosynthesis inhibition and during lignin biosynthesis *per se*, respectively [27,28]. Other cell wall-related genes include two genes encoding xyloglucan endotransglucosylase/hydrolase (XTH) 25 (HORVU7Hr1G098280 and HORVU7Hr1G098260) and barley *Low Silicon Influx 1* (*HvLSI1*; *HORVU6Hr1G075850*) [29], both downregulated in the mutant. These cell wall-related genes may support *COM1* involvement in regulation of cell wall mechanics of palea cells and the IM-to-SM boundary, and indirectly, putative signaling required for acquiring SM identity.

Discussion

Here we report that barley COM1 affects cell growth through regulation of cell wall properties specifically in palea and IM-to-SM boundary cells; the latter provide identity signals to barley SMs [30]. Signaling to the SM to establish its identity is a key genetic switch by which barley inflorescences acquire spike architecture, not seen in non-*Triticeae* grasses.

COM1 is present only in grasses, with no true *Arabidopsis* ortholog; intriguingly, we observed functional modification of COM1 between barley and non-*Triticeae* grass species. The modification in COM1 function was clear by comparing mutant versus wild type inflorescence phenotypes across grass species, and was further elucidated by our analysis at the cellular/molecular level. At the phenotypic level, barley COM1 inhibits spike-branching to simplify floral architecture; whereas in non-*Triticeae* COM1 homologs promote formation of lateral branches (e.g. up to 60% more branches in maize when compared to mutants [18]) to sustain the ancestral inflorescence complexity.

At the cellular level in non-*Triticeae* grasses, COM1 has evolved as a boundary formation factor, its putative ancestral role (**Fig. 5C-D**). Consequently, loss-of-function of COM1 homologs result in lack of boundaries and subsequent organ fusion, e.g. BM into IM as demonstrated by a

low number of lateral branches in maize mutants. Notably, this loss of function did not change the overall inflorescence architecture in non-*Triticeae* grasses. Barley *com1* loss-of-function, however, increases branch formation/extension mostly from SMs, a clear deviation from the canonical spike form. As barley *COM1* displayed a similar boundary mRNA expression as seen in maize, we presume that barley COM1 functions through boundary signaling [30], thereby affecting the identity of adjacent SMs. The formation of boundary regions in barley *com1* mutants (no organ fusion) via pathway(s) independent of *COM1* (**Fig. 5E-F**), and thus separation of meristematic zones in this mutant, implies that barley IM-to-SM boundary cells fail to deliver proper identity-defining signals to SMs. This signaling failure may perturb transcriptional programs required to establish identity in barley SMs; such meristems eventually revert back to IM-like meristems forming a branch-like structure (**Fig. 5F)**. The function of the boundary, and boundary-expressed genes (e.g., maize *RAMOSA1–3*), as a signaling center for adjacent meristems, e.g. SMs, has been proposed in grasses, yet features of these signals remain unknown [30]. Signals associated with COM1 might include micromechanical forces derived from formation of rigid cell walls enclosing boundary cells. Involvement of COM1 in printing such mechanical regulation is supported by our anatomical analysis of palea cell walls and further confirmed by our transcriptome analysis of immature barley spike samples. *HvLG1*, *HvLSI* and genes encoding one LRR-RLK, one CYP450 and two XTHs were among the most downregulated in the mutant and involved in defining cell wall properties [26-28,31]. The contribution of boundary cell wall mechanics in guiding organogenesis within reproductive tissues has been well described in dicot species [32].

Such functional modification usually includes constraints on expression patterns, protein sequence/structure or participation in molecular networks, often assumed to be associated with gene duplication [21]. Notably, *COM1* shows no sign of duplication within the barley genome and

as mentioned above displays a similar expression pattern to maize [17,18]. Thus, COM1's functional modification and implication in boundary-derived signaling seem to be associated with its protein sequence (**Fig. 2D**) and the respective downstream molecular networks. Furthermore, COM1's role in regulating floral complexity-levels in grasses fits well with the view that TCP transcription factors are growth regulators and evolutionary architects of plant forms that create diversity [33]. They influence the final architecture of plants in response to endogenous and/or external conditions. Thus, the barley floral reductionism (from compound spike to spike form; **Fig. 1A-D**) contributed by COM1, might be a response to the ecological expansion of the *Triticeae* into more temperate climates [3].

In summary, our findings enabled identification of a barley SM identity module, *VRS4* (*HvRA2*) → *COM1* → *HvLG1*, which works independently of *COM2* and inhibits spike-branching via boundary-defined signals (**Fig. 5A and Supplementary Fig. 12**). Our model of branch-inhibition in barley spikes opens a new window into grass inflorescence evolution and molecular crop breeding, and the elevated grain number per spike in *com1.a/com2.g* double mutants supports this notion.

Methods

Barley Plant material

The Nordic Genetic Resource center, the National Small Grains Collection (US Department of Agriculture), and the IPK gene bank were inquired to access 'Compositum-Barley' mutants (Supplementary Table 4). Bowman near isogenic line carrying *com1.a* allele ((i.e., BW-NIL(*com1.a*); syn. BW189 or CIho 11333)), its two-rowed progenitor Foma and Wt barley cv. Bowman were used for phenotypic descriptions, whole genome shotgun sequencing (WGS) (see

below) as well as SEM analysis. Plant material used to generate mapping populations is reported in the corresponding section for genetic mapping. For haplotype analysis, a core collection including of 146 diverse barley landraces and 90 diverse wild barleys were sequenced [24,25] (Supplementary Table 6).

Plant phenotyping

Barley; For phenotyping the mapping population, barley BW-NIL(*com1.a*) , Bowman and the corresponding segregating populations (F_2 and F_3) were grown side by side under greenhouse conditions at the IPK. For a plant to be assigned as a branched spike mutant, spike shape at all tillers was visually inspected for presence of at least one extra spikelet at any rachis node. Grain related characters such as weight, number, etc. were also measured at harvest for the two parental lines of the mapping population. In case of phenotyping of the barley TILLING population (see below and the Supplementary Table 4), other induced mutants (Supplementary Table 4) as well as the BW-NIL(*com1.a*) / BW-NIL(*com2.g*) double mutants (see below), visual phenotyping for variation in palea structure was also applied in addition to the aforementioned phenotyping approach used for spike branching in F_2 and F_3 progenies. In case of TILLING, from the six mutants for which the spike-branching phenotype was observed at M4, only three (carrying mutation inside the protein domain; M4.15104, M4.4406, and M4. 2598) were subjected for further study at M5 generation. For which, one M4 plant was selected from which 16 M5 plants were grown and phenotyped.

***Brachypodium distachyon**:* An already published TILLING population and the corresponding Wt accession Bd21-3 were used for phenotyping [34]. That included measurement of branch angle, as proxy for pulvinus size, spikelet number per spike, floret number per spikelet and palea structure.

Hence, per M4 plants, only homozygous M5 plants either with mutant genotype aa (3 to 4 plants) or wild type bb (3 to 4 plants) were selected. Per M5 plants, 10 M6 plants were grown under greenhouse conditions at the IPK and used for measurement. Thus, 30 to 40 plants per group and for each plant angles of basal spikelets in main tillers were considered for measurement. To this end, spikes were first imaged and then imported to the ImageJ tool (https://imagej.nih.gov/ij/index.html) for angle measurement. In case of original wild type Bd21-3, five plants were grown and measured. The same set of plants and the corresponding spike images were used to calculate number of spikelets per spike and number of floret per spikelet. In case of palea phenotyping: paleae were visually inspected across all spikes per plant. We detected plants with paleae being sensitive to exogenous finger-pressure, and thus such plants were scored as mutants. A gentle finger-pressure led the mutant paleae to crash from the middle longitude-line so that a scissors-like structure was formed (Fig. 3G). The crashing was not evident in Wt plants even with severe exogenous hand-pressure.

Sorghum: An already published TILLING population and the corresponding Wt accession BTx623 were used for phenotyping [35]. To measure primary branch number and angle, 5 to 8 plants, either M5 or M6 generations, per family including a Wt sorghum family cv. BTx623 were grown under greenhouse conditions at the IPK. Average branch number per panicle, e.g. per plant, was calculated by counting all branches that originated per each rachis node (Supplementary Table 5). The Average branch number per family was then used to compare with the same value obtained from Wt family BTx623. To measure the branch angle, for each plant 3 to 4 basal nodes per panicle were separately photographed. Each node contained at least 1 and up to 5 lateral branches. To cover angles of each individual branch per node, each node was photographed multiple time. Images

were then imported to ImageJ for angle measurement as described for *Brachypodium* (see above). Spikelet organs of palea and glume as well as overall grain set were also visually inspected for any visible alteration.

Marker development

Bowman near isogenic line BW-NIL(*com1.a*) and two-rowed progenitor of *com1.a,* cv. Foma, were survey sequenced using WGS approach (see below). These sequence information were compared against already available WGS of Bowmann [36], as present in **Supplementary Fig. 1**. Polymorphisms e.g. SNPs detected from this comparison (named as Next Generation Sequencing based markers (NGS-based markers)) between the two parental lines were converted to restriction enzyme based CAPS (http://nc2.neb.com/NEBcutter2/) markers to derive a restriction based genetic marker as previously described [12]. The developed genetic markers (**Supplementary Table 1**) were used to screen the corresponding mapping population.

Genetic mapping and map-based cloning of *com1.a*

com1.a was initially proposed to be located in chromosome 5HL with unknown genetic position [11]. A barley F_2 mapping population was developed by crossing Bowman introgression line BW-NIL(*com1.a*) and barley cv. Bowman. For initial mapping 180 individuals were analyzed and genotyped using the aforementioned NGS based markers. The pattern of segregation between mutant and Wt F_2 plants fitted a 3:1 ratio typical for a monogenic recessive gene. Linkage analysis of segregation data was carried out using maximum likelihood algorithm of Joinmap 4.0. Kosambi mapping function was used to convert recombination fractions into map distances. The linkage

mapping was further followed by a high-resolution genetic mapping in which almost 6,000 gametes were screened with the flanking markers NGS045 and NGS049. For narrowing down the *com1.a* genetic interval; the identified recombinants (a set of 109) were used. From 109, a set 15 F_2 were labeled (**Supplementary Table 2-3**) to be critical recombinants for precisely defining the *com1.a* genetic interval. From each of the 15 critical plants, 16 F_3 progenies were evaluated for their phenotypes and marker genotypes at the *com1.a* candidate gene. (**Supplementary Table 2 and S3**). Based on F_2 high-resolution mapping and F_3 genetic analysis described, two tightly linked markers, NGS084 and NGS094, were taken to harvest the available barley genome BAC sequence data (data not shown). A single BAC contig spanning 1.4 Mb of the minimal tiling path (MTP) was identified. Genes in this region were utilized for marker development and further genetic mapping that resulted in identification of a ~380 kb region deleted in the mutant BW-NIL(*com1.a*). The deleted fragment contains a single gene, i.e., *com1.a*.

Allelism test of *com1* mutants.

Mut.3906 mutant (**Supplementary Table 4**) was crossed with BW-NIL(*com1.a*) to test for allelism. The resultant F_1 plants showed a mutant spike phenotype confirming its allelism with *com1*. All alleles showed phenotypic similarities with *com1* and mutations in the *COM1* gene sequences.

Double-mutant analysis

Double mutants (DM) were generated by crossing mutant BW-NIL(*com1.a*) to BW-NIL(*com2.g*), followed by selfing of the F_1 progeny. All obtained 183 F_2 plants were subsequently genotyped

412 (**Supplementary Table 1**). In case of *com2.g* mutation detection, a primer pair (Com2-
413 Bw_SfiI_FR; **Supplementary Table 1**) spanning the A300C haplotype (that differentiate the Wt
414 Bowman allele A from *com2*.g mutant C allele at position 300bp [12] were used for sequencing and
415 to classify F_2 genotypes for the *com2* locus. Thus, genotypic classes include C300C allele as
416 homozygous mutant, AA as Wt and CA as heterozygous. In case of *com1.a*, a presence/absence
417 marker was used (**Supplementary Table 1**), where absence of the *COM1* gene was considered as
418 homozygous *com1.a* mutant. A total number of five plants were recovered as homozygous double
419 mutants (from 183 F_2 plants) (Supplementary Note) that were used for generating F_3 plants used in
420 subsequent DM phenotypic analysis (**Supplementary Fig. 6**). Two DM F_3 families, each
421 consisting of 20 plants along with 20 plants from each of the single mutants and 20 wild type cv.
422 Bowman plants, were grown and used for phenotyping (**Supplementary Fig. 5 and 6**).

423

424 **TILLING analysis**

425 **Barley:** For identifying further mutant alleles of *COM1* in barley TILLING populations including
426 EMS (Ethyl methanesulfonate) treated population of cv. Barke consisting 10279 individuals were
427 screened [37]. A primer combination (**Supplementary Table 1**) was used to amplify the coding
428 region of the *COM1* gene. The amplicon was subjected to standard procedures using the
429 AdvanCETM TILLING kit as described in [12]. Amplified products were digested with dsDNA
430 cleavage kit followed by analysis via mutation discovery kit and gel-dsDNA reagent kit. These
431 were performed on the AdvanCETM FS96 system according to manufacturer's guidelines
432 (advancedanalytical, IA, USA). The amplified ORF was also re-sequenced by Sanger sequencing
433 using primers listed in **Supplementary Table 1**.

Brachypodium distachyon: Mutation detection screenings were performed in the TILLING collection of chemically induced *Brachypodium* mutants, described in [34]. TILLING by NGS consists to sequence 500 bp PCR fragments libraries prepared from 2600 individual genomic DNA pooled in two dimensions. A dual indexing system, one placed on the 5'adaptater, and the second one on the 3'adaptater, added by a two-step PCR (for primer sequence; see **Supplementary Table 1**) allow a direct identification of the sequence identities. The first PCR amplification is a standard PCR with target-specific primers carrying Illumina's tail (**Supplementary Table 1**) and 10 ng of *Brachypodium* genomic DNA. Two microliter of the first PCR product served as a template for the second PCR amplification, with a combination of Illumina indexed primers (**Supplementary Table 1**). The sequencing step of PCR fragments was done on an Illumina Miseq personal sequencer using the MiSeq Reagent Kit v3 (Illumina®) followed by quality control processes for libraries using the PippinHT system from SAGE Sciences for libraries purification, and the Bioanalyzer™ system from Agilent®. To identify induced mutations, a bioinformatic pipeline, called "Sentinel" was used to analyze the data sequences (IDDN.FR.001.240004.000.R.P.2016.000.10000). Prediction of the impact of each mutation (**Supplementary Table 4**) was made with SIFT software as described in in [34]. The amplified ORF was also re-sequenced by Sanger sequencing using primers listed in **Supplementary Table 1**.

Sorghum: A pedigreed sorghum mutant library was established in the inbred line BTx623, which was used to produce the sorghum reference genome. This mutant library consists of 6400 M4 seed pools derived from EMS-treated sorghum seeds by single seed descent. Whole genome sequencing of a set of 256 lines uncovered 1.8 million canonical EMS-induced mutations [34]. We searched the sorghum ortholog of the barley *COM1* in the aforementioned sequence database to identity plants carrying mutation. To confirm the mutations, the amplified ORF was also re-sequenced by Sanger sequencing using primers listed in Supplementary Table 1.

458 **Haplotype and network analysis**

459 Genomic DNA from a core collection including 146 landrace and intermedium barley accessions
460 as well as 90 wild barley (Supplementary Table 6) was PCR-amplified using specific primers to
461 amplify full coding sequence of the barley *COM1* gene. Amplified fragments were used for direct
462 PCR sequencing (Sanger method; BigDye Terminator v3.1 cycle sequencing kit; Applied
463 Biosystems). A capillary-based ABI3730xl sequencing system (Applied Biosystems) at the
464 sequencing facility of IPK was used to separate the fluorescently terminated extension products.
465 Sequence assembly was performed using Sequencher 5.2.2.3. Visual inspection of sequence
466 chromatograms was carried out using Sequencher to detect the corresponding SNPs. Network
467 analysis of the nucleotide haplotypes was carried out using TCS v1.21 software
468 (http://darwin.uvigo.es/software/tcs.html) [38].

469

470 **RNA extraction, sequencing and data analysis**

471 **RNA Extraction;** For the RNA-seq study, immature spike tissues were collected from BW-
472 NIL(*com1.a*) and WT progenitor Bowman and the donor cultivar Foma. Plants were grown
473 under phytochamber conditions of 12h light (12 ºC) and 12h dark (8 ºC). Tissues were always
474 collected at the same time slot (14:00 to 17:00) during the day at three different developmental
475 stages including TM and GP, and pooled stages of LP+SP. Three biological replicated were
476 applied that resulted in 27 individual tissue samples. The TRIzol method (Invitrogen) was applied
477 to extract total RNA from immature spike tissues followed by removal of genomic DNA
478 contamination using RNAse-free DNAse (Invitrogen). RNA integrity and quantities were analyzed
479 via Agilent 2100 Bioanalyzer (Agilent Technologies) and Qubit (Invitrogen), respectively.

Preparation and sequencing of mRNA-Seq libraries: SENSE mRNA-Seq libraries (27 = 3 reps/3 stages /3 genotype) were prepared from 2 µg total RNA according to the protocol provided by the manufacturer (Lexogen GmbH, Vienna, Austria). Libraries were pooled in an equimolar manner and analysed electrophoretially using the Agilent 4200 TapeStation System (Agilent Technologies, Inc., Santa Clara, CA, USA). Quantification of libraries and sequencing (rapid run, paired-end sequencing, 2 x 100 cycles, on-board clustering) using the Illumina HiSeq2500 device (Illumina, San Diego, California, USA) were as described previously [39].

Analysis of the RNAseq data:

The reads from all three biological replicates were pooled per stage and each pool was independently mapped to barley pseudomolecules [36], (160404_barley_pseudomolecules_masked.fasta) using TopHAT2 [40]. Gene expression was estimated as read counts for each gene locus with the help of featureCounts [41] using the gene annotation file Hv_IBSC_PGSB_r1_HighConf.gtf and fragment per million (FPM) values were extracted from the BWA-aligned reads using Salmon [42]. Genes that showed FPM of 0 across all 45 samples were excluded from expression levels calculations. Expression levels were normalized by TMM method and *p*-values were calculated by an exact negative binomial test along with the gene-specific variations estimated by empirical Bayes method in edgeR [43]. The Benjamini-Hochberg method was applied on the *p*-values to calculate *q*-values and to control the false discovery rate (FDR). Differentially expressed genes (DEGs) were defined as *q*-value < 0.05, log2 fold change > 1 or < -1.

Quantitative RT-PCR

Tissue sampling, RNA extraction, qualification and quantification was performed as described above. Reverse transcription and cDNA synthesis were carried out using SuperScript III Reverse Transcriptase kit (Invitrogen). Real-time PCR was performed using QuantiTect SYBR green PCR kit (Qiagen) and the ABI prism 7900HT sequence detection system (Applied Biosystems). Each qRT-PCR comprised at least four technical replicates, and each sample was represented by three biological replicates. The *Actin* gene based primers (**Supplementary Table 1**) were used as the reference sequence. qRT-PCR results were analyzed using SDS2.2 tool (Applied Biosystems) in which the presence of a unique PCR product was verified by dissociation analysis. Significance values were calculated using Student's *t*-test (two-tailed). The relevant primer sequences per species are detailed in **Supplementary Table 1**.

Phylogenetic analysis

A comprehensive analysis of TCP proteins in grasses was already available we therefore focused only on constructing a detailed phylogeny of the COM1 protein among grasses and the barley TCP genes. Thus, barley COM1 was then queried against Ensembl Plants database to retrieve its orthologs or homologs from other grasses. The same database was also used to extract all barley TCP proteins. In case of COM1, protein and DNA sequence of the first and the second best hit (FBHs and SBHs) to each of the grass species were retrieved. To re-check their homology with barley COM1, the retrieved sequences were blasted back against the barley genome. For phylogenetic analysis, protein sequences were initially aligned using the algorithm implemented in CLC sequence viewer V7.8.1 (https://www.qiagenbioinformatics.com). UPGMA tree construction method and the distance measure of Jukes-Cantor were implemented for constructing the

phylogenetic tree using CLC sequence viewer. The bootstrap consensus tree inferred from 1000 replicates was taken to represent the evolutionary relationship of the sequences analyzed.

mRNA in situ hybridization

Three separated segments (excluding the TCP domain) from the *COM1* gene each containing 300-360 bp were synthesized (probe 1 and 2, GenScript Biotech , Netherlands) or amplified (probe 3) using cDNAs isolated from immature spikes of cv. Bonus and specific primers (Supplementary Table 1). The resulting products were cloned into pBluescript II KS (+) vector (Stratagene, La Jolla, CA, USA and GenScript Biotech , Netherlands). Linearized clones by HindIII or NotI were used as templates to generate antisense (HindIII) and sense (NotI) probes using T3 or T7 RNA polymerase. *In situ* hybridization was conducted with a single pool of the three aforementioned probes as described previously [44].

Scanning electron microscopy

Scanning electron microscopy (SEM) was performed on immature spike tissues at five stages including triple mound, glume, lemma, stamen, and awn primordium from greenhouse-grown plants. SEM was conducted as described elsewhere [45].

DNA preparation

DNA was extracted from leaf samples at the seedling as described before [12]. Plants for which the DNA was prepared included barley, *Sorghum* and *Barchypodium*. That included either mapping population, TILLING mutants or both.

545 **Palea anatomical and transmission electron microscopy analyses.**

546 Plant material consisting of intact spikes shortly before anthesis was collected. Spikelets containing
547 no grains were used for dissecting paleae that were subsequently stored in fixative (4% FA, 1%
548 GA in 50 mM phosphate buffer). Central spikelets (in case of barley) were isolated and placed in
549 a 15 ml test tube containing 10 ml fixative, followed by extensive degassing until all probes had
550 settled. Material was stored in a fridge until use. After three washes with A.D., lemma and palea
551 were isolated by cutting away a small part at the base of the spikelet. Isolated paleae were placed
552 in a flat bottomed mould filled with 4% liquid agarose (~60°C). After setting, agarose blocks were
553 removed from the mold and the encapsuled Palea was cut into 1-2mm wide sections using fresh
554 razor blades. The embedding in agarose facilitated the cuttings while preventing unnecessary
555 damage to the probes. After embedding in Spurr resin (see next page) semithin sections of 2 µm
556 were cut on an Leica Ultracut. Sections were allowed to be baked in on a droplet of 0,02%
557 Methylene blue/Azur blue on a heating plate set at 90°C. Recordings were made using a Keyence
558 VHX-5000 digital microscope (Keyence Germany GmbH, Neu-Isenburg, Germany).

559

560 **Sequence information and analysis**

561 Unpublished sequence information for the BAC contigs 44150 spanning the interval between
562 NGS084 and NGS094) was made available from the international barley sequencing consortium
563 (through Nils Stein). This sequence information was used for marker development during high
564 resolution mapping, map-based cloning and *COM1* gene identification. Later on, the initial contigs
565 44150 sequence information was re- checked and confirmed with the higher-quality barley genome
566 assembly and annotation data [23].

Whole genome shotgun sequencing of BW-NIL (*com1.a)*

A whole-genome shotgun library was constructed using standard procedures (TruSeq DNA; Illumina) and quantified using real-time PCR. Cluster formation using the cBot device and paired-end sequencing (HiSeq2000, 2 x 101 cycles) were performed according to the manufacturer's instructions (Illumina).

590 **References**

591 1. Zhang, D.B. & Yuan, Z. Molecular Control of Grass Inflorescence Development. *Annual*
592 *Review of Plant Biology, Vol 65* **65**, 553-78 (2014).
593
594 2. Vegetti, A. & Anton, A.M. Some Evolution Trends in the Inflorescence of Poaceae. in
595 *Flora* Vol. 190 225-228 (1995).
596
597 3. Kellogg, E.A. *et al.* Early inflorescence development in the grasses (Poaceae). *Frontiers*
598 *in Plant Science* **4** (2013).
599
600 4. Endress, P.K. Disentangling confusions in inflorescence morphology: Patterns and
601 diversity of reproductive shoot ramification in angiosperms. *Journal of Systematics*
602 *and Evolution* **48**, 225-239 (2010).
603
604 5. Remizowa, M.V., Rudall, P.J., Choob, V.V. & Sokoloff, D.D. Racemose inflorescences of
605 monocots: structural and morphogenetic interaction at the flower/inflorescence
606 level. *Annals of Botany* **112**, 1553-1566 (2013).
607
608 6. Kellogg, E.A. Evolutionary history of the grasses. *Plant Physiology* **125**, 1198-1205
609 (2001).
610
611 7. Koppolu, R. & Schnurbusch, T. Developmental pathways for shaping spike
612 inflorescence architecture in barley and wheat. *J Integr Plant Biol* **61**, 278-295 (2019).
613
614 8. Lemmon, Z.H. *et al.* The evolution of inflorescence diversity in the nightshades and
615 heterochrony during meristem maturation. *Genome Research* **26**, 1676-1686 (2016).
616
617 9. Malcomber, S.T., Preston, J.C., Reinheimer, R., Kossuth, J. & Kellogg, E.A. Developmental
618 gene evolution and the origin of grass inflorescence diversity. *Advances in Botanical*
619 *Research: Incorporating Advances in Plant Pathology, Vol 44* **44**, 425-481 (2006).
620
621 10. Vollbrecht, E., Springer, P.S., Goh, L., Buckler, E.S. & Martienssen, R. Architecture of
622 floral branch systems in maize and related grasses. *Nature* **436**, 1119-1126 (2005).
623
624 11. Druka, A. *et al.* Genetic dissection of barley morphology and development. *Plant*
625 *Physiol* **155**, 617-27 (2011).
626
627 12. Poursarebani, N. *et al.* The Genetic Basis of Composite Spike Form in Barley and
628 'Miracle-Wheat'. *Genetics* **201**, 155-165 (2015).
629
630 13. Cosgrove, D. Biophysical Control of Plant-Cell Growth. *Annual Review of Plant*
631 *Physiology and Plant Molecular Biology* **37**, 377-405 (1986).
632

14. Cosgrove, D.J. Plant cell wall extensibility: connecting plant cell growth with cell wall structure, mechanics, and the action of wall-modifying enzymes. *Journal of Experimental Botany* **67**, 463-476 (2016).
15. Martin-Trillo, M. & Cubas, P. TCP genes: a family snapshot ten years later. *Trends Plant Sci* **15**, 31-9 (2010).
16. Zhao, J. *et al.* Genome-Wide Identification and Expression Profiling of the TCP Family Genes in Spike and Grain Development of Wheat (Triticum aestivum L.). *Frontiers in Plant Science* **9** (2018).
17. Lewis, M.W. *et al.* Gene regulatory interactions at lateral organ boundaries in maize. *Development* **141**, 4590-4597 (2014).
18. Bai, F., Reinheimer, R., Durantini, D., Kellogg, E.A. & Schmidt, R.J. TCP transcription factor, BRANCH ANGLE DEFECTIVE 1 (BAD1), is required for normal tassel branch angle formation in maize. *Proceedings of the National Academy of Sciences of the United States of America* **109**, 12225-12230 (2012).
19. Zeng, D.-D. *et al.* DBOP specifies palea development by suppressing the expansion of the margin of palea in rice. *Genes & Genomics* **38**, 1095-1103 (2016).
20. Yuan, Z. *et al.* RETARDED PALEA1 Controls Palea Development and Floral Zygomorphy in Rice. *Plant Physiology* **149**, 235-244 (2009).
21. Studer, R.A. & Robinson-Rechavi, M. How confident can we be that orthologs are similar, but paralogs differ? *Trends in Genetics* **25**, 210-216 (2009).
22. Jiao, Y.P. *et al.* MSD1 regulates pedicellate spikelet fertility in sorghum through the jasmonic acid pathway. *Nature Communications* **9** (2018).
23. Aguilar-Martinez, J.A., Poza-Carrion, C. & Cubas, P. Arabidopsis BRANCHED1 acts as an integrator of branching signals within axillary buds. *Plant Cell* **19**, 458-472 (2007).
24. Koppolu, R. *et al. Six-rowed spike4* (*Vrs4*) controls spikelet determinacy and row-type in barley. *Proceedings of the National Academy of Sciences of the United States of America* **110**, 13198-13203 (2013).
25. Russell, J. *et al.* Exome sequencing of geographically diverse barley landraces and wild relatives gives insights into environmental adaptation. *Nature Genetics* **48**, 1024-1030 (2016).
26. Liu, K. *et al.* Wheat TaSPL8 Modulates Leaf Angle Through Auxin and Brassinosteroid Signaling. *Plant Physiology* **181**, 179-194 (2019).

27. Van der Does, D. *et al.* The Arabidopsis leucine-rich repeat receptor kinase MIK2/LRR-KISS connects cell wall integrity sensing, root growth and response to abiotic and biotic stresses. *Plos Genetics* **13** (2017).

28. Gou, M.Y., Ran, X.Z., Martin, D.W. & Liu, C.J. The scaffold proteins of lignin biosynthetic cytochrome P450 enzymes. *Nature Plants* **4**, 299-310 (2018).

29. Chiba, Y., Mitani, N., Yamaji, N. & Ma, J.F. HvLsi1 is a silicon influx transporter in barley. *Plant Journal* **57**, 810-818 (2009).

30. Whipple, C.J. Grass inflorescence architecture and evolution: the origin of novel signaling centers. *New Phytol* **216**, 367-372 (2017).

31. Hara, Y., Yokoyama, R., Osakabe, K., Toki, S. & Nishitani, K. Function of xyloglucan endotransglucosylase/hydrolases in rice. *Annals of Botany* **114**, 1309-1318 (2014).

32. Landrein, B. & Ingram, G. Connected through the force: mechanical signals in plant development. *Journal of Experimental Botany* **70**, 3507-3519 (2019).

33. Manassero, N.G., Viola, I.L., Welchen, E. & Gonzalez, D.H. TCP transcription factors: architectures of plant form. *Biomol Concepts* **4**, 111-27 (2013).

34. Dalmais, M. *et al.* A TILLING Platform for Functional Genomics in Brachypodium distachyon. *PLoS One* **8**, e65503 (2013).

35. Jiao, Y.P. *et al.* A Sorghum Mutant Resource as an Efficient Platform for Gene Discovery in Grasses. *Plant Cell* **28**, 1551-1562 (2016).

36. Mascher, M. *et al.* A chromosome conformation capture ordered sequence of the barley genome. *Nature* **544**, 427 (2017).

37. Gottwald, S., Bauer, P., Komatsuda, T., Lundqvist, U. & Stein, N. TILLING in the two-rowed barley cultivar 'Barke' reveals preferred sites of functional diversity in the gene HvHox1. *BMC Res Notes* **2**, 258 (2009).

38. Clement, M., Posada, D. & Crandall, K.A. TCS: a computer program to estimate gene genealogies. *Mol Ecol* **9**, 1657-9 (2000).

39. Beier, S. *et al.* Construction of a map-based reference genome sequence for barley, Hordeum vulgare L. *Scientific Data* **4**, 170044 (2017).

40. Kim, D. *et al.* TopHat2: accurate alignment of transcriptomes in the presence of insertions, deletions and gene fusions. *Genome Biology* **14**, R36 (2013).

41. Liao, Y., Smyth, G.K. & Shi, W. featureCounts: an efficient general purpose program for assigning sequence reads to genomic features. *Bioinformatics* **30**, 923-930 (2014).

42. Patro, R., Duggal, G., Love, M.I., Irizarry, R.A. & Kingsford, C. Salmon provides fast and bias-aware quantification of transcript expression. *Nature Methods* **14**, 417-419 (2017).

43. Robinson, M.D., McCarthy, D.J. & Smyth, G.K. edgeR: a Bioconductor package for differential expression analysis of digital gene expression data. *Bioinformatics* **26**, 139-140 (2010).

44. Komatsuda, T. *et al.* Six-rowed barley originated from a mutation in a homeodomain-leucine zipper I-class homeobox gene. *Proceedings of the National Academy of Sciences of the United States of America* **104**, 1424-1429 (2007).

45. Lolas, I.B. *et al.* The transcript elongation factor FACT affects Arabidopsis vegetative and reproductive development and genetically interacts with HUB1/2. *Plant J* **61**, 686-97 (2010).

Acknowledgments: We thank the US Department of Agriculture–Agricultural Research Service (USDA-ARS), the National Small Grains Collection, Aberdeen (ID); the Nordic Genetic Resources Center (NordGen), Alnarp, Sweden; and the IPK Genebank, Germany, for providing the mutants and germplasm for haplotype analysis. The authors would like to thank Dr. Shun Sakuma for fruitful discussions and help in conducting mRNA *in-situ* hybridizations. We are thankful to Dr. Marion Dalmais, INRA Evry, France, for providing access to and screening of the *Brachypodium distachyon* TILLING resource, Anne Fiebig for help with data submission to ENA and Sandra Driesslein, Jenny Knibbiche, Mechthild Pürschel, Ines Walde, Kerstin Wolf, Marion Benecke and Kirsten Hoffie for excellent technical assistance.

Funding: During this study, research in the Schnurbusch laboratory received financial support from the Federal Ministry of Education and Research (BMBF) FKZ 0315954A and 031B0201A, HEISENBERG Program of the German Research Foundation (DFG), grant No. SCHN 768/8-1 and SCHN 768/15-1, as well as IPK core budget.

Author contributions: T.S. conceived the idea for the study, designed and monitored experiments, and analyzed data. N.P. expanded the idea for the study, designed and performed experiments and analyzed data; C.T. executed the mRNA *in-situ* hybridizations. M.M. conducted microscopic analyses of cellular structures in paleae. T.N. analyzed RNA-seq data. U.L. provided irregular and intermedium barley spike mutants. T.R. executed SEM analyses. T.Schm. conducted sequence read mapping to unpublished barley genomic sequences for SNP calling. R.B., A.H. and L.A. performed the initial whole-genome shotgun sequencing of the parental genotypes for mapping. R.K. was involved in the phenotypic analysis of *com1.a* and RT-qPCR analyses of *COM1* in barley *vrs4* mutant. H.M.Y. provided sequences from a barley diversity panel for haplotype analysis and was involved in the RT-qPCR analysis. M.D. and A.B. provided the *Brachypodium* TILLING resource; N.S. provided the barley TILLING resource; Z.X. provided the sorghum TILLING resource. N.P. and T.S. wrote the manuscript including contributions from co-authors. All authors have seen and agreed upon the final version of the manuscript.

Competing interests:

The authors declare no conflict of interest.

Data and materials availability:

Barley mutants are available from TS under a material transfer agreement (MTA) with IPK-Gatersleben. All data are available in the main text or online materials. The RNA-seq data and the whole genome shotgun (WGS) sequences of *com1.a* mutant have been submitted to the European

Nucleotide Archive under accession number PRJEB35746 and PRJEB35761, respectively. COM1 sequences are available with the corresponding ID mentioned in the current study in the public databases https://plants.ensembl.org/ & https://apex.ipk-gatersleben.de/apex/f?p=284:10 and are in the process of submission to NCBI as well.

Figure Legends:

Main Figures

Fig. 1 Proposed evolutionary pattern of grass inflorescences, and the spike/palea morphology of wild-type and *com1.a* mutant barley. (**A–D**) Model for grass inflorescence evolution from ancestral compound form to spike in *Triticeae*; re-drawn from [2]. (**E**) Spike morphology of wild-type (Wt) barley *cv*. Bowman. **(F–G**) Branched (mutant) BW-NIL(*com1.a*). (**H–I**) Floral reversion of spikelet to small spike-like branch structure from severe (**H**) to weak appearance as an extended rachilla (**I**). (**J–M**) Consecutive developmental stages of immature BW-NIL(*com1.a*) mutant spike from early glume primordium (**J**), advanced glume primordium (**K**), to advanced lemma (**L**) and early stamen primordium (**M**). (**N**) Dorsal view of immature BW-NIL(*com1.a*) mutant spike at early stamen primordia. (**O)** Longitudinal adaxial palea view of the BW-NIL(*com1.a*); white rectangle corresponds to the area used to take sections for histological analysis and to the lower image depicting the flat-plane surface of a cross section. (P) Longitudinal adaxial view of Wt palea; the lower image corresponds to the infolding surface of a cross section. (**Q–R**) Histological analyses of transverse sections (from O and P; white rectangles) of palea in mutant (**Q**) and Wt (**R**). Paleae are from spikelets shortly before anthesis. (**S–Z**) Walls of palea cells in mutant (**S-V**) versus Wt (**W-Z**).

Fig. 2 Map-based cloning of the gene underlying *com1.a*, phylogenetic analysis and protein structural variation of COM1. (**A**) Physical and genetic maps of *com1.a* from 100 recombinant plants or ~6,000 gametes. A single gene (red; HORVU5Hr1G061270, a single-exon TCP transcription factor) was the strongest candidate and deleted in the mutant parent BW-NIL(*com1.a*). (**B**) *COM1* gene model containing one TCP DNA binding domain. Six TILLING alleles are shown with prefix M3 (**Supplementary Note**). **(C)** UPGMA phylogenetic tree, using 1000 bootstrap replications, of COM1 first best (highlighted in gray) and second best homologs. (**D**) Evolutionarily conserved motifs among proteins present in the phylogenetic tree using SALAD. (see also **Supplementary Fig. 8**).

Fig. 3 Inflorescence morphology and gene expression patterns in sorghum (A–F) and *Brachypodium* (G–R). (**A**) Inflorescence shape in wild type (Wt) *cv*. BT623. (**B**). Compact inflorescence in TILLING mutant ARS180. (**C**) Expanded branch angle of Wt. (**D**) Acute branch angle in mutant ARS180. (**E**) Dissected dorsal view of the pulvinus (red circles). (**F**) RT-qPCR of *SbBad1/Wab1* in organs of Wt plants. 1_1, 1_2 and 1_3 represent first, second and third branch meristem stages, respectively. **(G)** Mutant palea scissor-like structure collapses easily due to external mechanical pressure; **(H)** normal/solid palea structure in Wt plants. **(I)** Acute branch angle in mutant **(J)**; expanded branch angle in Wt. (**K**) SEM view of transverse section of Wt palea; mutant has extra VB in middle **(L)** lacking in Wt **(M)**. (**N**) RT-qPCR of *BdBad1/Wab1* gene expression in Wt. **(O)** Branch angle measurement, as proxy for pulvinus size, among contrasting M6 homozygous TILLING lines; aa and bb refer to mutant and Wt homozygous, respectively (**Supplementary Note**). Values above x-axis indicate number of angles measured. **(P–Q)** were

used for measuring number of spikelets per individual inflorescence (panicle) (**P**) and number of florets per spikelet **(Q)** in the same M6 TILLING plant material (illustrated in **O**); mutants (gray boxes) showed no significant difference to Wt. P values were determined using *Student's t* test. Values above x-axis indicate number of plants**.** Genotype IDs below x-axis refer to the parental line of the respective M6 family.

Fig. 4. Transcript analyses of *COM1* in two-rowed barley. . **(A)** Relative *COM1* expression at different stages of immature spike and (**B)** organs along with spike sections (basal, central and apical at AP) of *cv*. Bowman.. Despite expression in tiller buds, no difference in tiller number was observed (**Supplementary Note, Supplementary Fig. 5**). y-axis value: expression relative to *HvActin*. (**C)** Semi-qPCR of *COM1* mRNA. **(D)** Control hybridization using sense probe. (**E–G**) mRNA in-situ hybridization of *COM1* in two-rowed Wt barley *cv*. Bonus. Tissues represent cross-section through a spikelet triplet at TM **(E)** and AP stages (**F–G**).

Fig. 5. Model of *COM1* regulation based on transcriptome analysis in barley (A–B) and schematic representation of *COM1* functional modification from non-*Triticeae* (C–D). Wt *COM1* transcriptional regulation model based on downregulation of the Wt allele. **(B)** RNA-seq-based heat map of selected differentially expressed (DE) genes; for the remaining DE genes see **Supplementary Fig. 11**. **(C–D)** IM-to-BM boundary formation due to Wt gene function (**C**) and lack of boundary due to the loss-of-function allele (**D**) in non-*Triticeae* grasses. Of note, *COM1* involvement in thickening the boundary cell walls within *non-Triticeae* species cannot be excluded. (**E**) IM-to-SM boundary formation in Wt barley; restriction of *COM1* function to cell wall thickening (the blue program), due to the evolutionary functional modification. (**F**). SM-to-IM

843 floral reversion observed in barley *com1.a* due to lack of the corresponding wall-amplified

844 micromechanical signals needed to confer SM identify.

845

Table1. Functional variation of *COM1* homologs observed among grass species

		Effect on the corresponding organ/meristem				
Species	Gene function in boundary	On branch formation	On pulvinus size/formation	Growth of palea cells	Number of VB [1] in palea	Pollen fertility[2]
Barley	signaling	Inhibition	- [3]	Inhibition[4]	Promotion	Normal
Brachypodium	formation[5]	No effect	Promotion	No effect [6]	Promotion	Normal
Rice	formation	Not known[7]	Promotion	Promotion	Promotion	Reduced
Sorghum	formation	Promotion	Promotion	No effect	Promotion	Reduced
Maize	formation	Promotion	Promotion	No effect	Not known	Not known

1 stands for Vasculature Bundles

2 revealed by grain setting measurements as a proxy

3 pulvinus is typically absent in Wt spike of *Triticeae* including barley as well as in the branched mutant spikes.

4 apparent at the longitudinally-middle palea part resulting in formation of the infloded area

5 Refers to the formation of boundary between pulvinus and the lateral branch without which fusion of the two happened. Reflects intermediate evolutionary phylogenetic positon of *Brachypodium* among grasses.

6 not visible at the microscopic level

7 perhaps because the rice cultivars used in the corresponding studies (*cv*. Nipponbare and *cv*. 9522) are known to exhibit panicles with acute lateral branches.

846

847

848 Figure 1

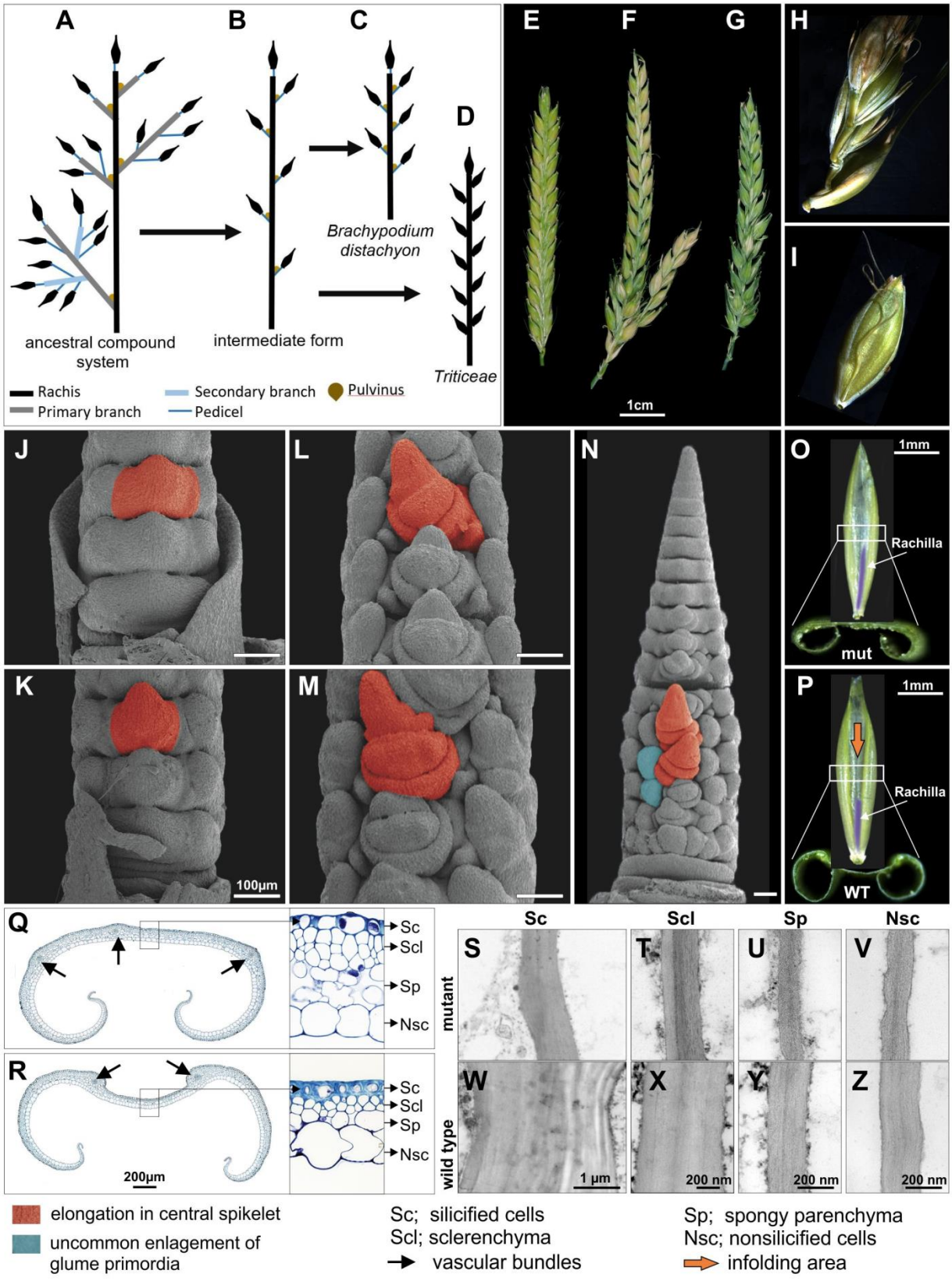

849

850 Figure 2

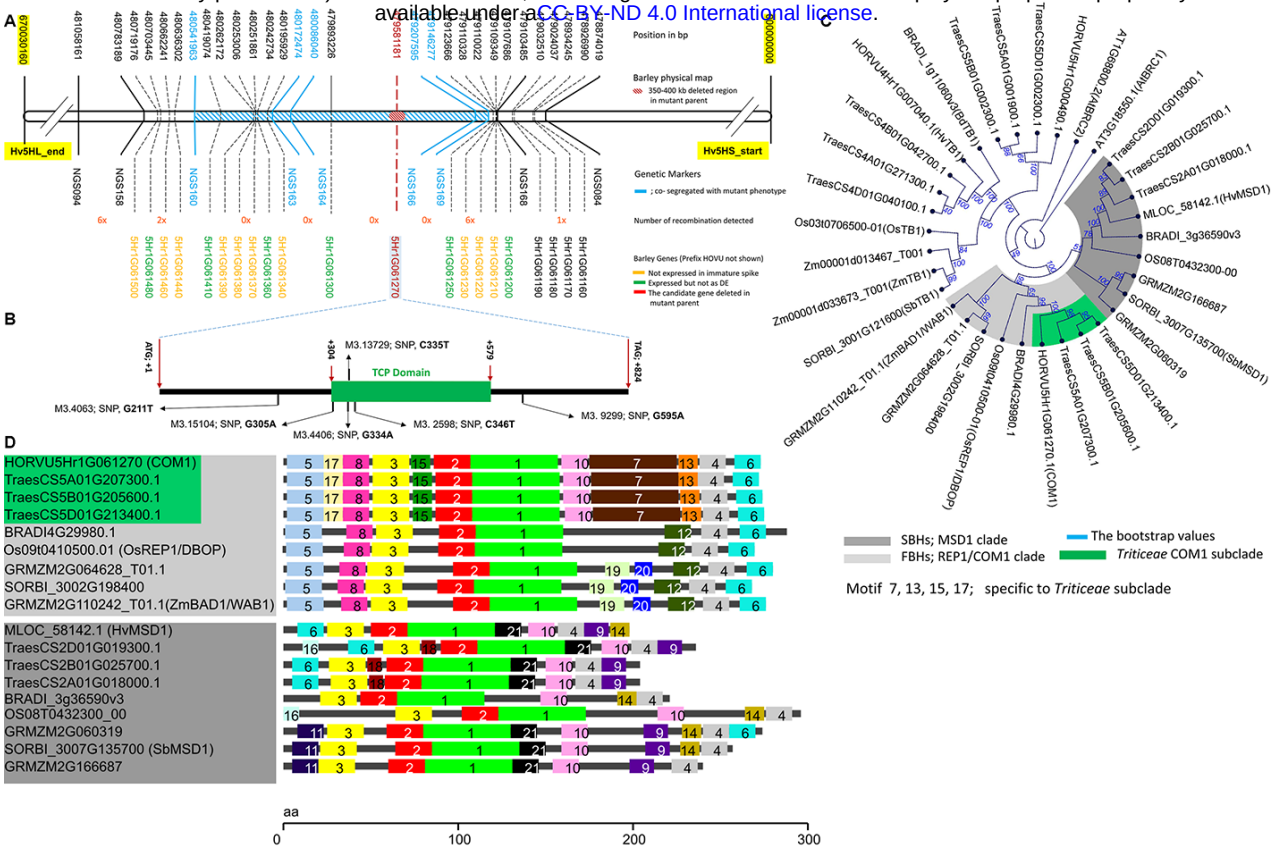

851

852

Figure 3

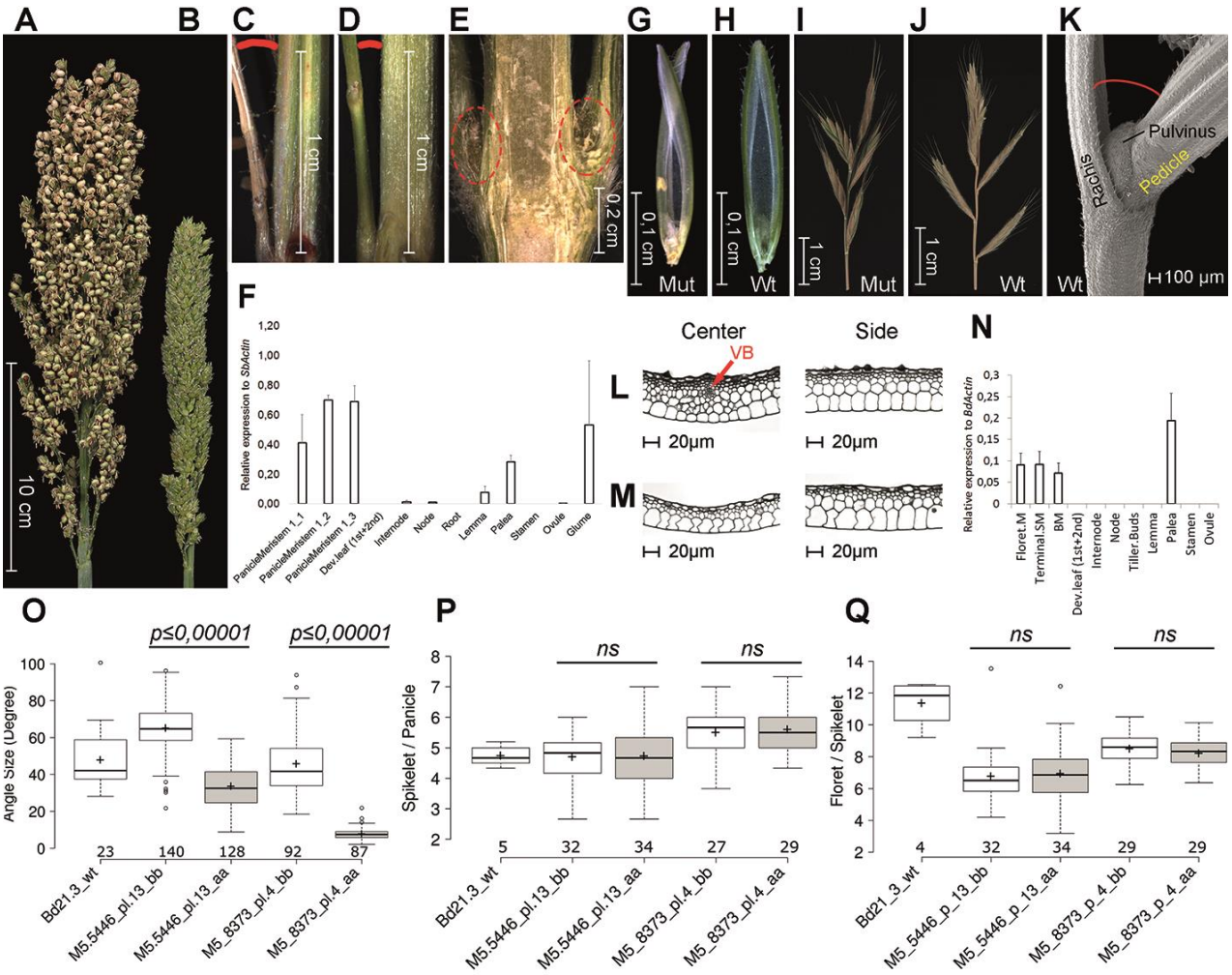

Figure 4

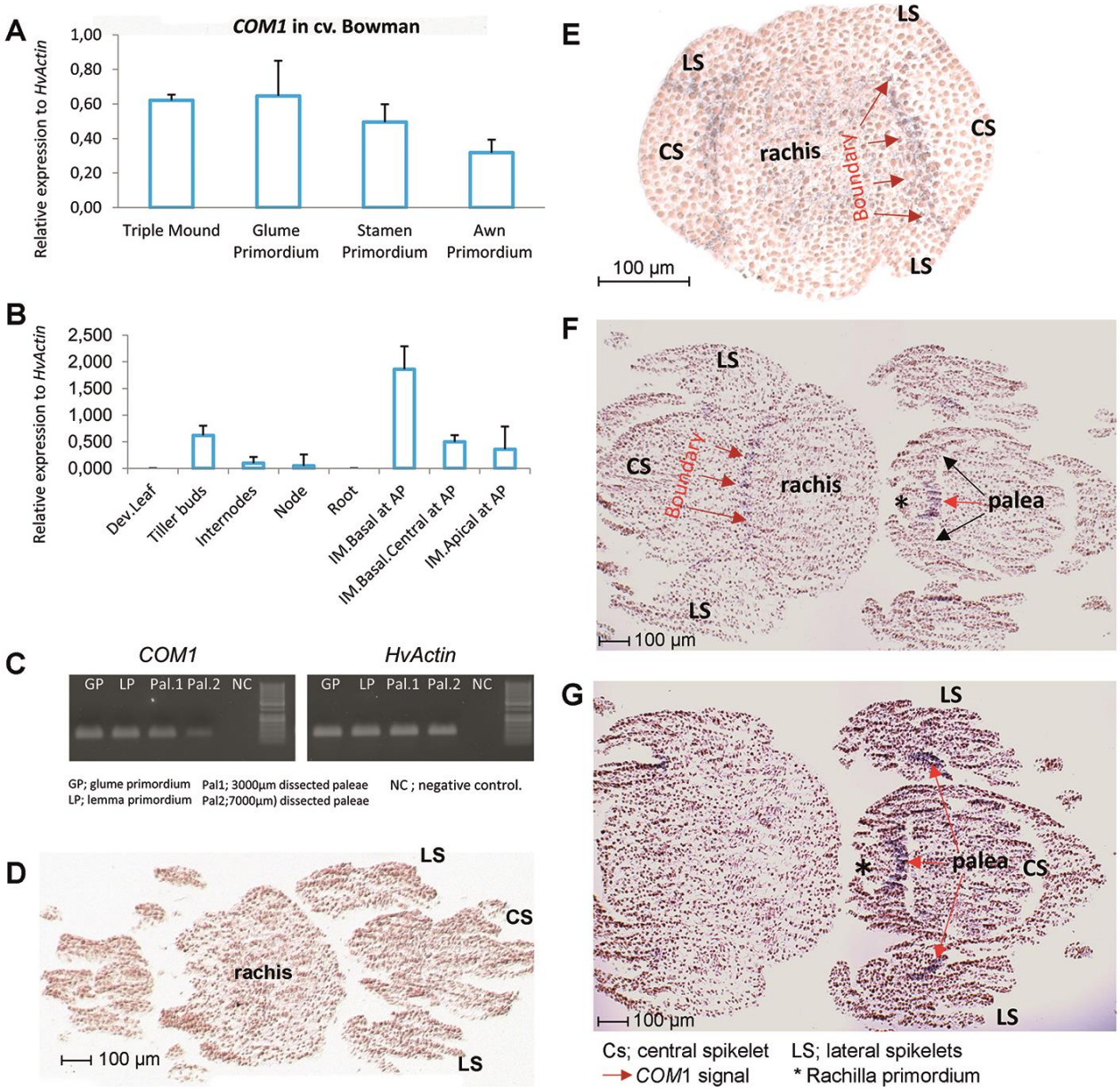

Figure 5

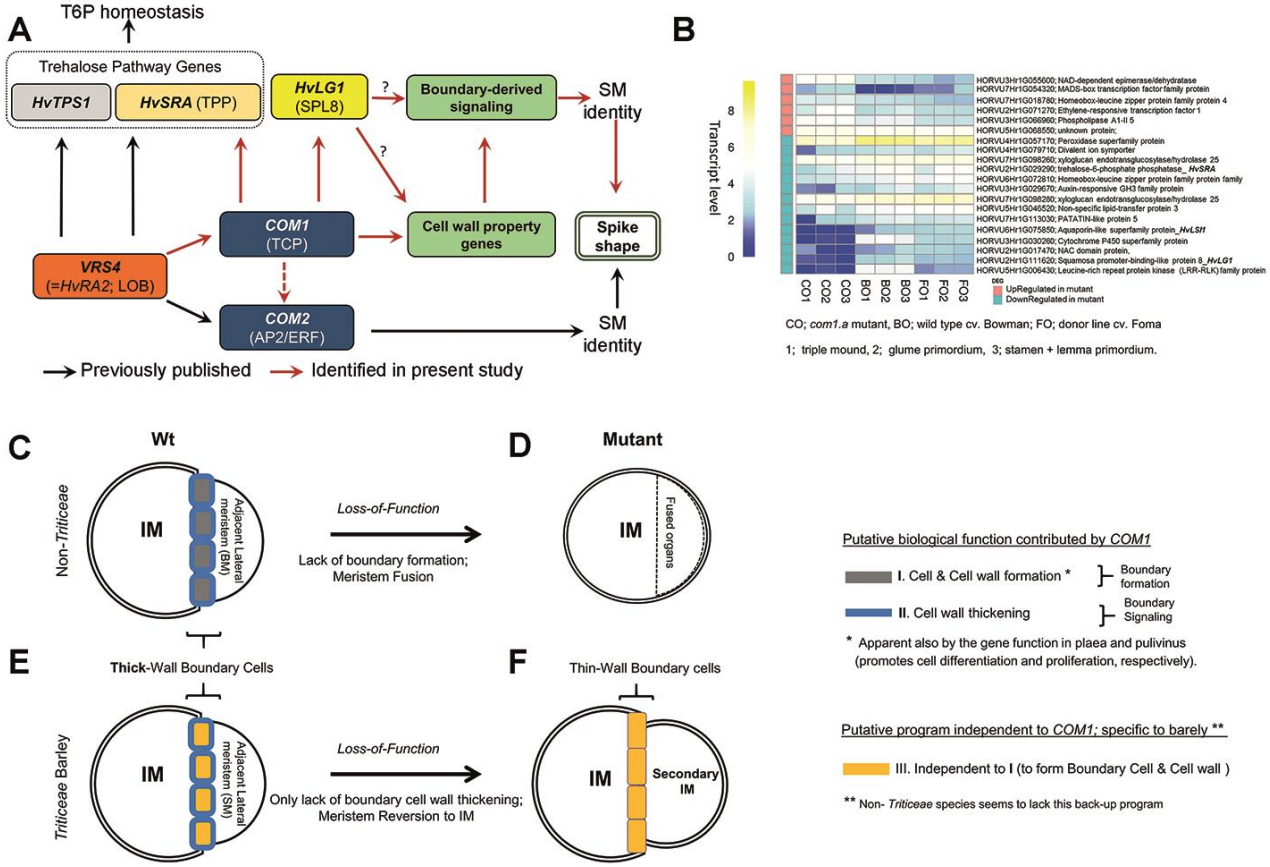

Supplementary Information for

Title:

COMPOSITUM 1 (COM1) contributes to the architectural simplification of barley inflorescence via cell wall-mediated and meristem identity signals

Authors:

N. Poursarebani[1], C. Trautewig[1], M. Melzer[1], T. Nussbaumer[3,4], U. Lundqvist[5], T. Rutten[1], T. Schmutzer[1,2], R. Brandt[1], A. Himmelbach[1], L. Altschmied[1], R. Koppolu[1], H. M. Youssef[1,2,6], M. Dalmais[7], A. Bendahmane[7], N. Stein[1], Z. Xin[8], T. Schnurbusch[1,2]

*Corresponding authors. Email: Poursarebani@ipk-gatersleben.de (NP); Schnurbusch@ipk-gatersleben.de (TS)

This file includes:

Supplementary Notes

References

Supplementary Figs. 1 to 12

Supplementary Tables 1 to 6

Captions for Supplementary Source Data 1

Supplementary Notes

COM1 positional cloning in barley

The genetic map was conducted by screening ~6,000 gametes for recombination events in an F_2 population (Bowman x *com1.a)*. After which, fifteen critical recombinant F_2-derived F_3 families (i.e., 16 plants per family; **Supplementary Table 2- 3**) were further analyzed that unambiguously confirmed the genetic interval detected. Resequencing a set of 20 barley spike-branching mutants, using both CDS and promoter specific primer pairs (**Supplementary Table 1 and S4**), revealed that five of them, i.e. *Mut.3906*, *int-h.42, int-h.43* and *int-h.44*, and *com1.i*, lost the same transcription factor as found missing in the *com1.a* mutant (**Supplementary Fig. 3, Supplementary Table 1 and 4**). All five mutants also showed the flat-palea phenotype observed in the mutant *com1.a* (**Supplementary Fig. 3**). Allelism tests of *com1.a* with *Mut.3906* indicated that they are allelic to each other. Furthermore, we PCR-screened a barley TILLING populations from cv. Barke (two-rowed) for the CDS of the candidate gene. Four homozygous M3 plants (M3.15104, M3.4406, M3.13729 and M3. 2598) carrying SNP mutations inside the DNA binding domain as well as two heterozygous M3 lines M3.4063 and M3.9299 with SNP mutation outside the domain were identified (**Fig. 2B**). All six SNP mutations caused amino acid substitution in conserved positions (**Fig. 2B**). They all transmitted a branched spike as was revealed by the phenotypes of the corresponding M4 and M5 homozygous plants (**Fig. 2B; Supplementary Fig. 4–5; Supplementary Table 4**). Interestingly, from the six TILLING mutants, only two, with mutation within the TCP domain, showed either a true flat-palea phenotype with a complete loss of the infolding (line 2598, exhibiting also the most severe branching), or only a mild change in the palea shape (line 4406) (**Supplementary Fig. 4**). Thus, penetrance of the mutant flat-palea phenotype depended on the type and position of the amino acids substitution (**Supplementary Fig. 4**, legend). Taken

908 together, these data indicate that the mutations in this transcription factor caused the two *com1*
909 phenotypes.
910
911 **Development and characterized of BW-NIL (*com1.a com2.g*) double mutants**
912 20 BW-NIL(*com1.a com2.g*) double mutants homozygote plants along with 20 plants from each
913 of the single mutants and 20 wild type cv. Bowman plants, were grown and used for
914 phenotyping. The DM plants out-performed either single mutants in supernumerary spikelet
915 and branch production and grain number per spike, which was elevated by ~50% in DMs as
916 compared to single mutants alone (**Supplementary Fig. 6 and 12**, legend). Notably, all tillers
917 from DMs showed both supernumerary spikelet formation and spike-branching phenotypes. In
918 addition to the ramification observed in central SMs, SEM analysis of DM plants also showed
919 floral reversion of the lateral SMs (**Supplementary Fig. 6**). Both events were highly penetrant
920 and pronounced in the DM's immature spikes that led 100% of the plant tillers to exhibit a DM-
921 specific enhanced spike-branching phenotype at maturity (**Supplementary Fig. 6 and 12**). The
922 uncommon enlargement of the glum primordia (Blue asterisk in Fig. 1O) was seen only in ~5%
923 of the tillers in single mutant *com1.a* whereas 100 % of the tillers in *com1.acom2.g* double
924 mutants showed this enlargement (**Supplementary Fig. 12**).
925
926 **TILLING analysis of *BdCOM1* in *Brachypodium***
927 Our TILLING analysis in *Brachypodium distachyon* revealed several mutations in the *BdCOM1*
928 homolog from which two (M4. 5446; Q116* and M4. 8373; S146N) with predicted severe
929 damages to the protein domain and function were phenotypically characterized
930 (**Supplementary Table 4**). Hence, per M4 plants, only homozygous M5 plants either with
931 mutant genotype aa (3 to 4 plants) or wild type bb (3 to 4 plants) were selected. Per M5 plants,
932 10 M6 plants were grown. The homozygote states of the corresponding M5 and M6 mutant
933 family transmitted a defect in palea structure (**Fig. 3**). In which, we always observed a palea

scissor-like structure in all florets in mutants, as it collapses easily due to external mechanical pressure. In contrast, palea in Wt never made such structure while applying same external hand-pressure. Histological analyses of the *Brachypodium* mutants' palea revealed no obvious change in cell expansion (**Fig. 4**).

References

1. Zhang, D.B. & Yuan, Z. Molecular Control of Grass Inflorescence Development. *Annual Review of Plant Biology, Vol 65* **65**, 553-78 (2014).
2. Vegetti, A. & Anton, A.M. Some Evolution Trends in the Inflorescence of Poaceae. in *Flora* Vol. 190 225-228 (1995).
3. Kellogg, E.A. *et al.* Early inflorescence development in the grasses (Poaceae). *Frontiers in Plant Science* **4**(2013).
4. Endress, P.K. Disentangling confusions in inflorescence morphology: Patterns and diversity of reproductive shoot ramification in angiosperms. *Journal of Systematics and Evolution* **48**, 225-239 (2010).
5. Remizowa, M.V., Rudall, P.J., Choob, V.V. & Sokoloff, D.D. Racemose inflorescences of monocots: structural and morphogenetic interaction at the flower/inflorescence level. *Annals of Botany* **112**, 1553-1566 (2013).
6. Kellogg, E.A. Evolutionary history of the grasses. *Plant Physiology* **125**, 1198-1205 (2001).
7. Koppolu, R. & Schnurbusch, T. Developmental pathways for shaping spike inflorescence architecture in barley and wheat. *J Integr Plant Biol* **61**, 278-295 (2019).
8. Lemmon, Z.H. *et al.* The evolution of inflorescence diversity in the nightshades and heterochrony during meristem maturation. *Genome Research* **26**, 1676-1686 (2016).
9. Malcomber, S.T., Preston, J.C., Reinheimer, R., Kossuth, J. & Kellogg, E.A. Developmental gene evolution and the origin of grass inflorescence diversity. *Advances in Botanical Research: Incorporating Advances in Plant Pathology, Vol 44* **44**, 425-481 (2006).
10. Vollbrecht, E., Springer, P.S., Goh, L., Buckler, E.S. & Martienssen, R. Architecture of floral branch systems in maize and related grasses. *Nature* **436**, 1119-1126 (2005).
11. Druka, A. *et al.* Genetic dissection of barley morphology and development. *Plant Physiol* **155**, 617-27 (2011).
12. Poursarebani, N. *et al.* The genetic basis of composite spike form in barley and 'Miracle-Wheat'. *Genetics* **201**, 155-165 (2015).
13. Cosgrove, D. Biophysical Control of Plant-Cell Growth. *Annual Review of Plant Physiology and Plant Molecular Biology* **37**, 377-405 (1986).
14. Cosgrove, D.J. Plant cell wall extensibility: connecting plant cell growth with cell wall structure, mechanics, and the action of wall-modifying enzymes. *Journal of Experimental Botany* **67**, 463-476 (2016).
15. Martin-Trillo, M. & Cubas, P. TCP genes: a family snapshot ten years later. *Trends Plant Sci* **15**, 31-9 (2010).

16. Zhao, J. *et al.* Genome-Wide Identification and Expression Profiling of the TCP Family Genes in Spike and Grain Development of Wheat (Triticum aestivum L.). *Frontiers in Plant Science* **9**(2018).
17. Lewis, M.W. *et al.* Gene regulatory interactions at lateral organ boundaries in maize. *Development* **141**, 4590-4597 (2014).
18. Bai, F., Reinheimer, R., Durantini, D., Kellogg, E.A. & Schmidt, R.J. TCP transcription factor, *BRANCH ANGLE DEFECTIVE 1* (*BAD1*), is required for normal tassel branch angle formation in maize. *Proceedings of the National Academy of Sciences of the United States of America* **109**, 12225-12230 (2012).
19. Zeng, D.-D. *et al.* DBOP specifies palea development by suppressing the expansion of the margin of palea in rice. *Genes & Genomics* **38**, 1095-1103 (2016).
20. Yuan, Z. *et al.* RETARDED PALEA1 Controls Palea Development and Floral Zygomorphy in Rice. *Plant Physiology* **149**, 235-244 (2009).
21. Studer, R.A. & Robinson-Rechavi, M. How confident can we be that orthologs are similar, but paralogs differ? *Trends in Genetics* **25**, 210-216 (2009).
22. Jiao, Y.P. *et al.* MSD1 regulates pedicellate spikelet fertility in sorghum through the jasmonic acid pathway. *Nature Communications* **9**(2018).
23. Aguilar-Martinez, J.A., Poza-Carrion, C. & Cubas, P. Arabidopsis BRANCHED1 acts as an integrator of branching signals within axillary buds. *Plant Cell* **19**, 458-472 (2007).
24. Koppolu, R. *et al. Six-rowed spike4* (*Vrs4*) controls spikelet determinacy and row-type in barley. *Proceedings of the National Academy of Sciences of the United States of America* **110**, 13198-13203 (2013).
25. Russell, J. *et al.* Exome sequencing of geographically diverse barley landraces and wild relatives gives insights into environmental adaptation. *Nature Genetics* **48**, 1024-+ (2016).
26. Liu, K. *et al.* Wheat TaSPL8 Modulates Leaf Angle Through Auxin and Brassinosteroid Signaling. *Plant Physiology* **181**, 179-194 (2019).
27. Van der Does, D. *et al.* The Arabidopsis leucine-rich repeat receptor kinase MIK2/LRR-KISS connects cell wall integrity sensing, root growth and response to abiotic and biotic stresses. *Plos Genetics* **13**(2017).
28. Gou, M.Y., Ran, X.Z., Martin, D.W. & Liu, C.J. The scaffold proteins of lignin biosynthetic cytochrome P450 enzymes. *Nature Plants* **4**, 299-310 (2018).
29. Chiba, Y., Mitani, N., Yamaji, N. & Ma, J.F. HvLsi1 is a silicon influx transporter in barley. *Plant Journal* **57**, 810-818 (2009).
30. Whipple, C.J. Grass inflorescence architecture and evolution: the origin of novel signaling centers. *New Phytol* **216**, 367-372 (2017).
31. Hara, Y., Yokoyama, R., Osakabe, K., Toki, S. & Nishitani, K. Function of xyloglucan endotransglucosylase/hydrolases in rice. *Annals of Botany* **114**, 1309-1318 (2014).
32. Landrein, B. & Ingram, G. Connected through the force: mechanical signals in plant development. *Journal of Experimental Botany* **70**, 3507-3519 (2019).
33. Manassero, N.G., Viola, I.L., Welchen, E. & Gonzalez, D.H. TCP transcription factors: architectures of plant form. *Biomol Concepts* **4**, 111-27 (2013).
34. Dalmais, M. *et al.* A TILLING Platform for Functional Genomics in Brachypodium distachyon. *PLoS One* **8**, e65503 (2013).
35. Jiao, Y.P. *et al.* A Sorghum Mutant Resource as an Efficient Platform for Gene Discovery in Grasses. *Plant Cell* **28**, 1551-1562 (2016).
36. Mascher, M. *et al.* A chromosome conformation capture ordered sequence of the barley genome. *Nature* **544**, 427 (2017).

37. Gottwald, S., Bauer, P., Komatsuda, T., Lundqvist, U. & Stein, N. TILLING in the two-rowed barley cultivar 'Barke' reveals preferred sites of functional diversity in the gene HvHox1. *BMC Res Notes* **2**, 258 (2009).
38. Clement, M., Posada, D. & Crandall, K.A. TCS: a computer program to estimate gene genealogies. *Mol Ecol* **9**, 1657-9 (2000).
39. Beier, S. *et al.* Construction of a map-based reference genome sequence for barley, Hordeum vulgare L. *Scientific Data* **4**, 170044 (2017).
40. Kim, D. *et al.* TopHat2: accurate alignment of transcriptomes in the presence of insertions, deletions and gene fusions. *Genome Biology* **14**, R36 (2013).
41. Liao, Y., Smyth, G.K. & Shi, W. featureCounts: an efficient general purpose program for assigning sequence reads to genomic features. *Bioinformatics* **30**, 923-930 (2014).
42. Patro, R., Duggal, G., Love, M.I., Irizarry, R.A. & Kingsford, C. Salmon provides fast and bias-aware quantification of transcript expression. *Nature Methods* **14**, 417-+ (2017).
43. Robinson, M.D., McCarthy, D.J. & Smyth, G.K. edgeR: a Bioconductor package for differential expression analysis of digital gene expression data. *Bioinformatics* **26**, 139-140 (2010).
44. Komatsuda, T. *et al.* Six-rowed barley originated from a mutation in a homeodomain-leucine zipper I-class homeobox gene. *Proceedings of the National Academy of Sciences of the United States of America* **104**, 1424-1429 (2007).
45. Lolas, I.B. *et al.* The transcript elongation factor FACT affects Arabidopsis vegetative and reproductive development and genetically interacts with HUB1/2. *Plant J* **61**, 686-97 (2010).
46. Cao, Y.Y. *et al.* Identification of Differential Expression Genes in Leaves of Rice (Oryza sativa L.) in Response to Heat Stress by cDNA-AFLP Analysis. *Biomed Research International* (2013).
47. Zhao, T. *et al.* Characterization and expression of 42 MADS-box genes in wheat (Triticum aestivum L.). *Molecular Genetics and Genomics* **276**, 334-350 (2006).
48. Masiero, S., Colombo, L., Grini, P.E., Schnittger, A. & Kater, M.M. The Emerging Importance of Type I MADS Box Transcription Factors for Plant Reproduction. *Plant Cell* **23**, 865-872 (2011).

Supplementary figures

Supplementary Figure 1. Creation of induced Bowman near isogenic line (NIL), mapping population, marker resource and the low-resolution linkage map of *com1.a* in barley. (**A and B**) The *com1.a* phenotype was introduced (after its induction in barley cv. Foma) into a two-rowed barley cv. Bowman by six time backcrosses as reported previously [11]. Green area in chromosome 5H corresponds to the introgressed genomic segment caring the underlying *com1.a* mutation. (**C**) The resulted BW near isogenic line (NIL) of *com1.a* allele; BW-NIL (*com1.a*) was crossed to cv. Bowman to generate F_2 population used in genetic mapping. (**D**) BW-NIL (*com1.a*) was whole genome shotgun (WGS) sequenced to 10x coverage (Online Materials) and compared with already published WGS of Bowman [36]. (**E**) Represents alignment of the BW-NIL (*com1.a*) sequence assembly against the physically localized Bowman WGS sequence contigs. The corresponding SNPs (that were used for marker development) derived from the 5H introgression segment are plotted in the outer circle. (**F**) Genetic linkage mapping of *com1.a* in barley, derived from the F_2 mapping population (see part C). SNPs derived from E located within the introgressed region, were used for marker development. Markers in red selected for high-resolution genetic mapping. A-B were performed and published previously [11]. C-F are entirely performed in the present study, except WGS of the wild type cv. Bowman.

Supplementary Figure 2: TEM based cell wall structure in wild type palea versus mutant *com1.a*.

Left-ide; cross section of wild type palea in which different cell positions (used to image the cell walls shown in right panel) across cell layers (see Fig. 1S-T for the layer IDs) are labeled. **Right-side**; Cell walls thickness in Wt is depicted compared with that of mutant for each position of A-I; labeled accordingly in Left panel. BW-NIL (*com2.g*) mutant, that is visually

similar in palea phenotype/structure with that of Wt cv. Bowman, were used here to compare with the mutant *com1.a*.

Supplementary Figure 3. Additional mutant alleles of spike branching in barley. Different *com1* induced mutant alleles identified by resequencing of primers correspond to CDS and potential promotor region of *COM1*. The corresponding palea is shown in the upper –right side of each spike image. See also **Supplementary Table** 1 and 4.

Supplementary Figure 4. Phenotype and COM1 protein sequence alignment in barley TILLING lines. (**A**) A representative display of branch formation of the six barley TILLING mutant plants derived from barley cv. Barke. The corresponding palea is shown in the upper – right side of each spike image. (**B**) Protein sequence alignment of the six mutants, some located within the corresponding TCP domain (the red box). Mutation pointed with red arrows show severe (dark red; M4.2598) and very mild (light red; M4.4406) palea phenotypes, while green arrows show mutation with no palea phenotype.

Supplementary Figure 5. Tillering related characters in barley TILLING lines. (A) Average tiller number and (**B**) spike number per plant of the three spike-branching barley TILLING lines are compared against wild type cv. Barke. This was performed to check whether *COM1* expression detected in tiller buds (**Fig. 4B**) play any role in tiller formation. Twenty plants were grown per genotype under greenhouse conditions. *P* values were determined using the Student's *t* test.

Supplementary Figure 6. Immature spike and yield related components in double mutant BW-NIL (com1.a/com2.g) (DM). (A) Lateral view of a DM immature spike at late GP stage. (**B-D**) Close-up and complete view of a DM immature spike; depict reversion of lateral and central SMs as well as glume primordium into the IM-like meristems. (**E-J**) Yield components of the DM plants, and the corresponding single mutants com1.a and com2.g in comparisons to the Wt cv. Bowman. Data are based on a single greenhouse-condition experiment and on averages of 20 plants (390 to 540 spikes) per phenotypic class.

Supplementary Figure 7. Phylogeny of barley TCP proteins and the phylogeny-based model of *COM1* evolution. (A) 1000 bootstraps based UPGMA phylogenetic tree of 22 barley TCP proteins. (**B).** Depicts origin and divergence of two (out-) paralogs of REP1/COM1 (α) and MSD1 (β*;* [22] clades from a common ancestor [16]. This divergence seems to happen after genome duplication in grass common ancestor and before the grass speciation (e.g. the separation of *Triticeae* from *Non-Triticeae* species). More importantly, in case of paralogs α clade; although the clade members showed no duplication (no in-paralogy) after speciation, except in maize (Fig. 2C; light-grey block), they have gone through a functional modification that separate *Non-Triticeae* function (α1) from that of *Triticeae* subclade (α2). Which, coincidentally, the respective modification separates inflorescence shapes between the two groups of grass plants by regulating contrasting phenotypes of formation versus inhibition of branches. Whether out-paralog β also differs in function among grass (to be as β1 and β2) remains to be investigated. So far, only functional characterization of β in sorghum, the *SbMsdI*, has been reported [22]. Lines in brown represent the speciation process.

Supplementary Figure 8. Amino acid sequence alignment of the COM1 homologs among grass. The green box shows the TCP domain conservation.

Supplementary Figure 9. Network analysis of *COM1*. Depicts grouping of 237 barley accessions (including 90 wild barleys) producing 12 haplotypes; comprising two main haplotypes: namely Hap1 (154 wild and landraces) and Hap2 (64 wild and landraces) with Hap1 being assigned as ancestral. The remaining 10 haplotypes, except Hap8 that contains two landraces comprised only wild barleys (16 accessions), independently raised from Hap1 during the course of evolution. Accessions representing each of the 12 haplotypes were grown and carefully inspected for the spike and palea phenotype for which no obvious phenotypic alteration was observed. Sequences were obtained using primers for the CDS region.

Supplementary Figure 10. Branch formation in *vrs4* mutant (*mul1.a*). (**A**) Mature spike of wild type progenitor cv. Montcalm with determinate triple spikelet meristem. (**B-D**) Mature spikes of *vrs4* mutant MC (*mul1.a*) showing various levels of branch proliferation at the spike base and middle portion of the spike. See also [12]. *COM1* **(E)** and *COM2* **(F)** transcripts in BW-NIL(*vrs4.k*) (red) and *com1.a* (green) mutants, respectively. Mean ±SE of three biological replicates. *P* values were determined using the *Student's t* test.

Supplementary Figure 11. Transcriptome analysis of *com1.a* using RNA seq. Heat map of all DE genes (found in RNA seq; n = 3 reps/3 stages /3 genotype) conjointly in the BW-NL (*com2.g*) as compared to the corresponding wild type cv. Bowman and cv. Foma. The scale bar at the top of the heat map indicates the transcript level of differentially regulated genes observed between wild type and mutant; blue color indicates down-regulation while red shows up-regulation. Of the highly upregulated genes in mutant *com1.a* was HORVU3Hr1G055600; NAD-dependent epimerase/dehydratase gene family; associated with increased growth [46]. Other highly upregulated genes involved in plant reproduction (HORVU7Hr1G054320;, type I MADS-box transcription factor family protein; [47,48], as well as the floral meristem determinacy

(HORVU7Hr1G018780; Homeobox-leucine zipper protein family protein 4; homology to HAT1 gene in *Arabidopsis thaliana*) [3]. Up regulation of these gene sets is fairly in line with the observed spike-branching phenotype of the mutant *com1.a*. See the main text; for illustration of the relevant genes that are downregulated in mutant.

Supplementary Figure 12. The extended model of *COM1* regulations. (**A**) Model of Wt *COM1* transcriptional regulation based on "down-regulation" of the Wt allele (**B**) The resulted spike phenotype (% of tiller per mutant plant) due to the respective gene(s) loss-of-funation. Data are based on a single greenhouse-condition experiment and on averages of 20 plants (390 to 540 spikes) per mutant class (*com1.a*, *com2.g* and the respective double mutants).

Supplementary figures

Supplementary Figure 1.

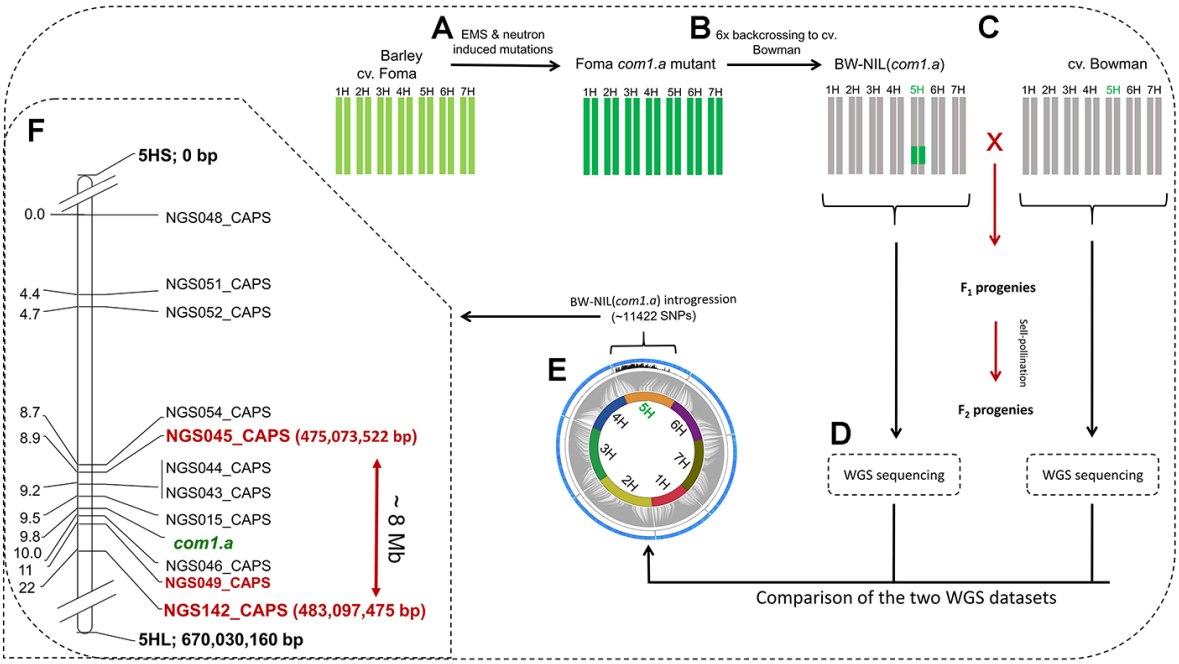

Supplementary Figure 2

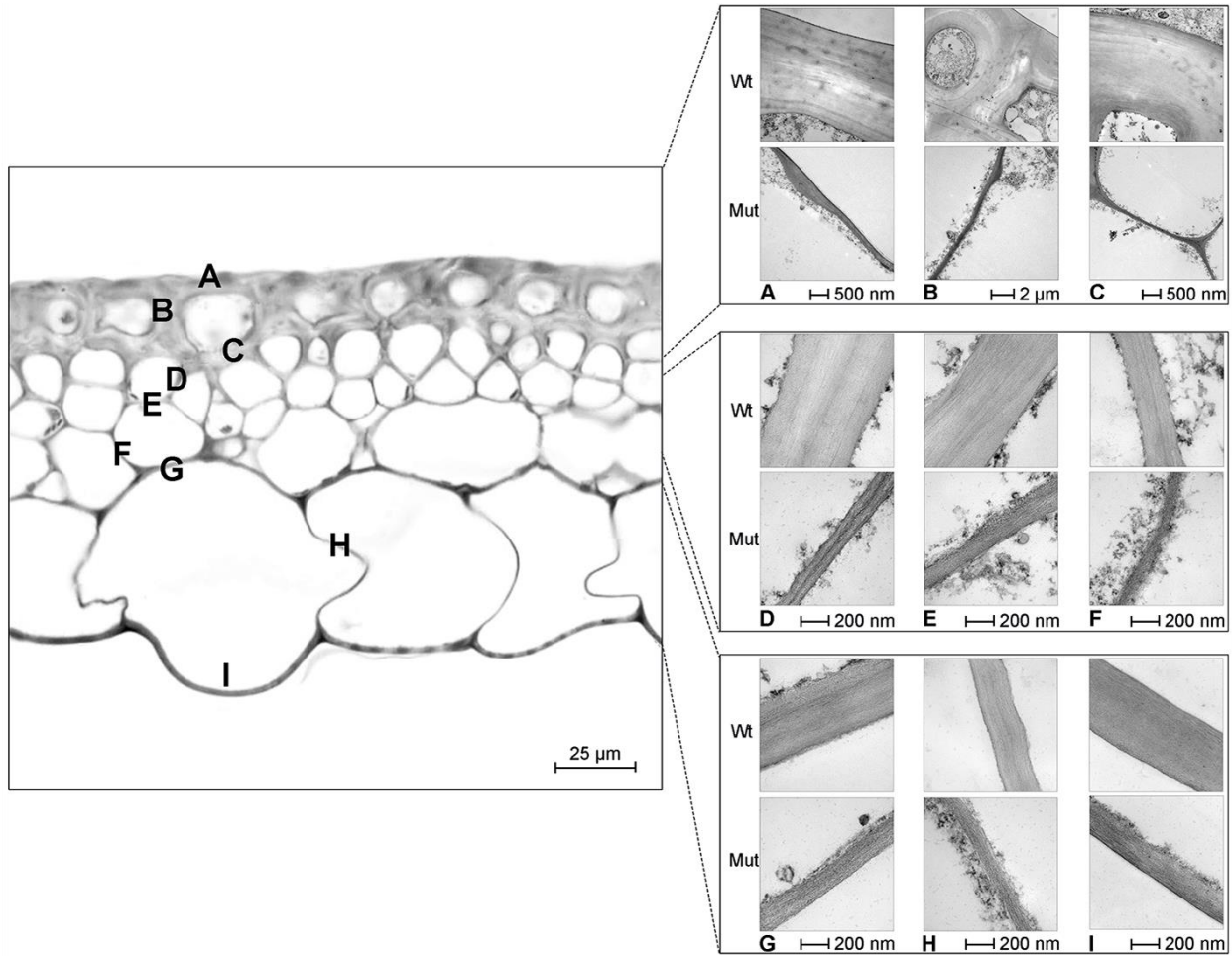

Supplementary Figure 3

Supplementary Figure 4

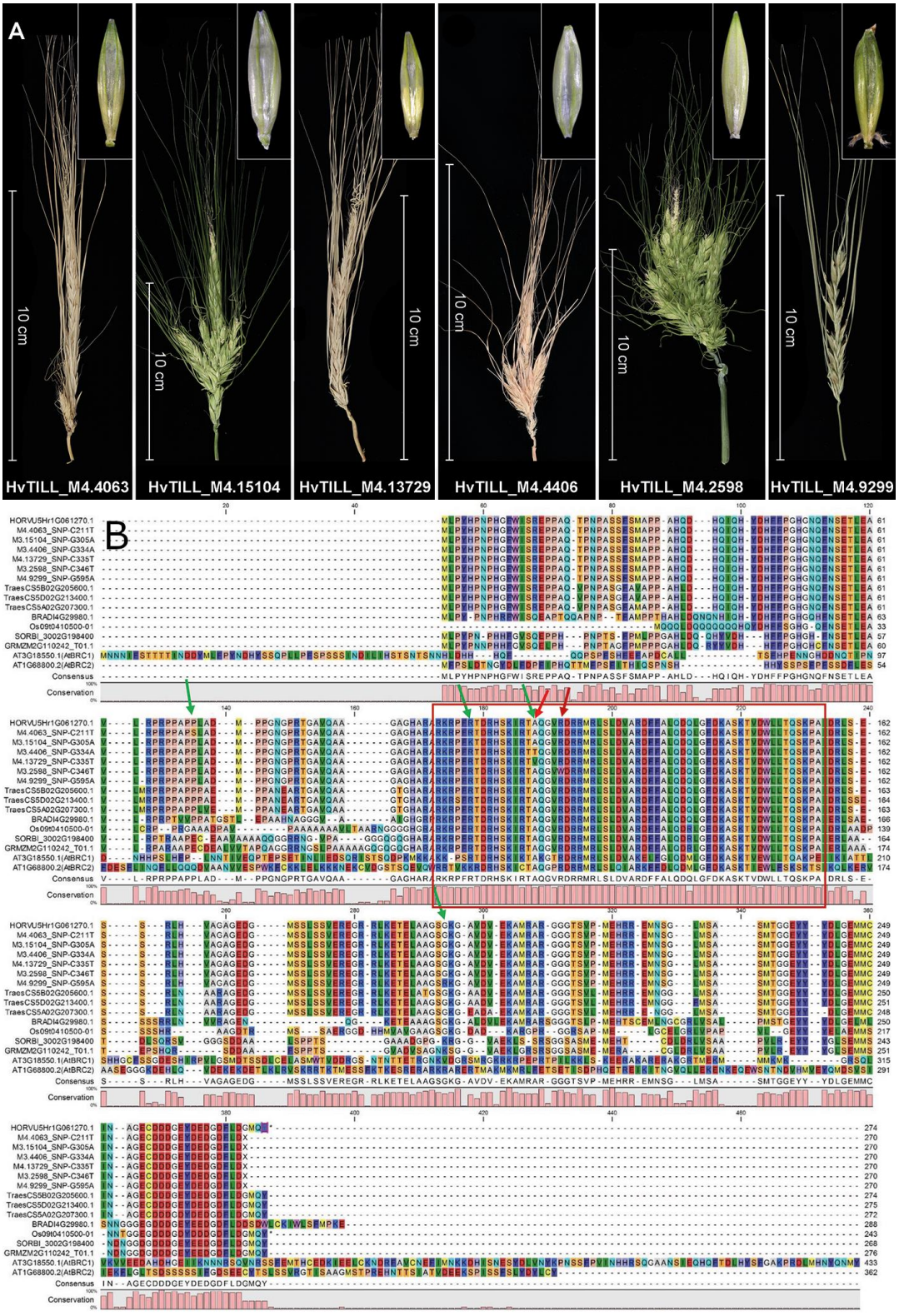

Supplementary Figure 5.

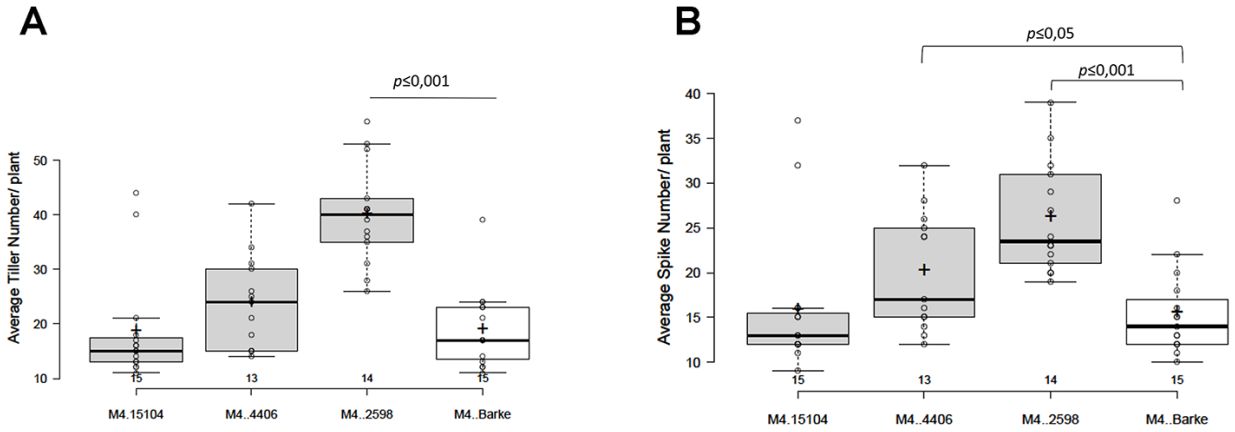

Supplementary Figure 6

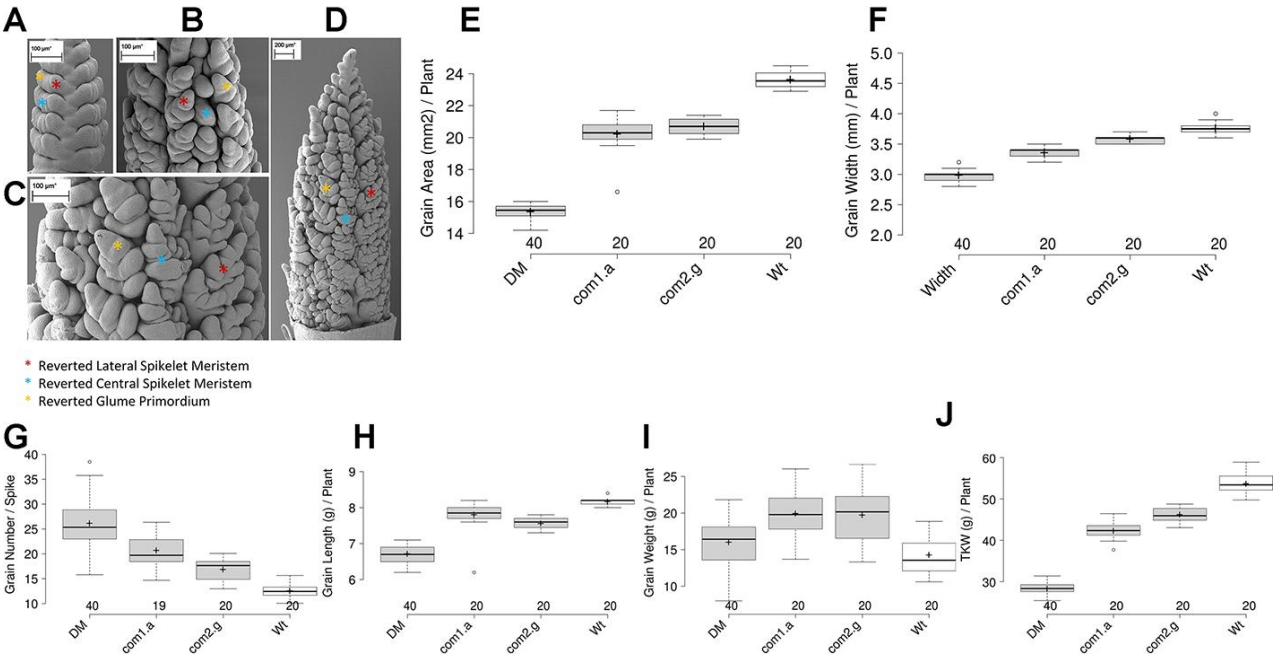

.

Supplementary Figure 7

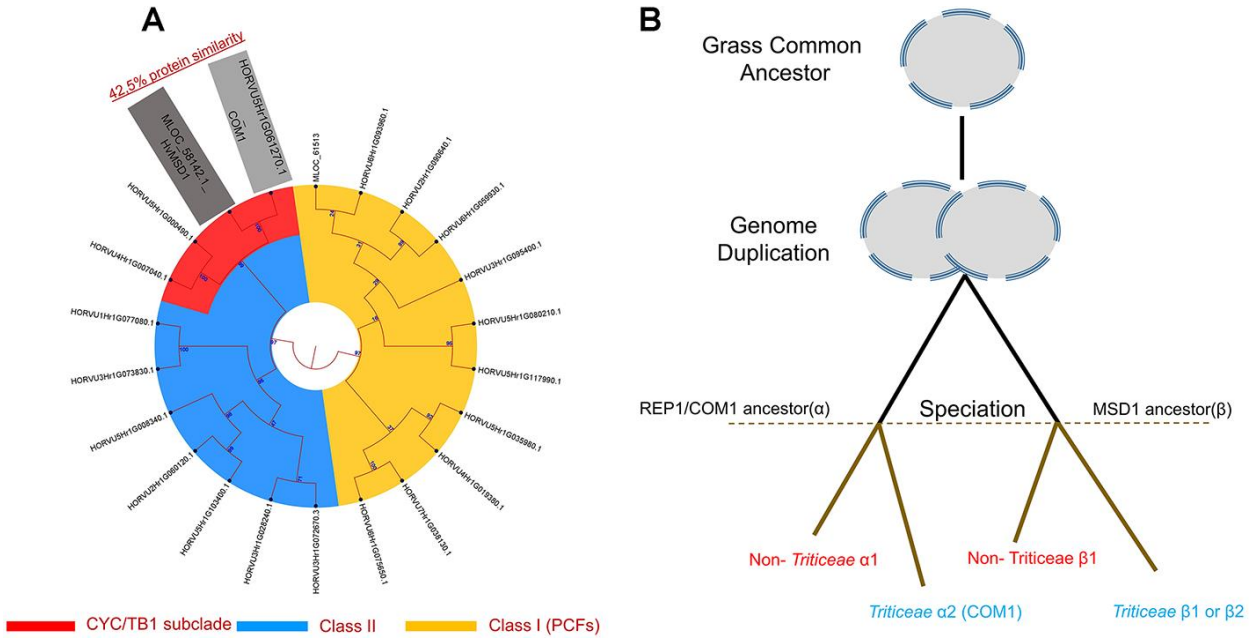

Supplementary Figure 8

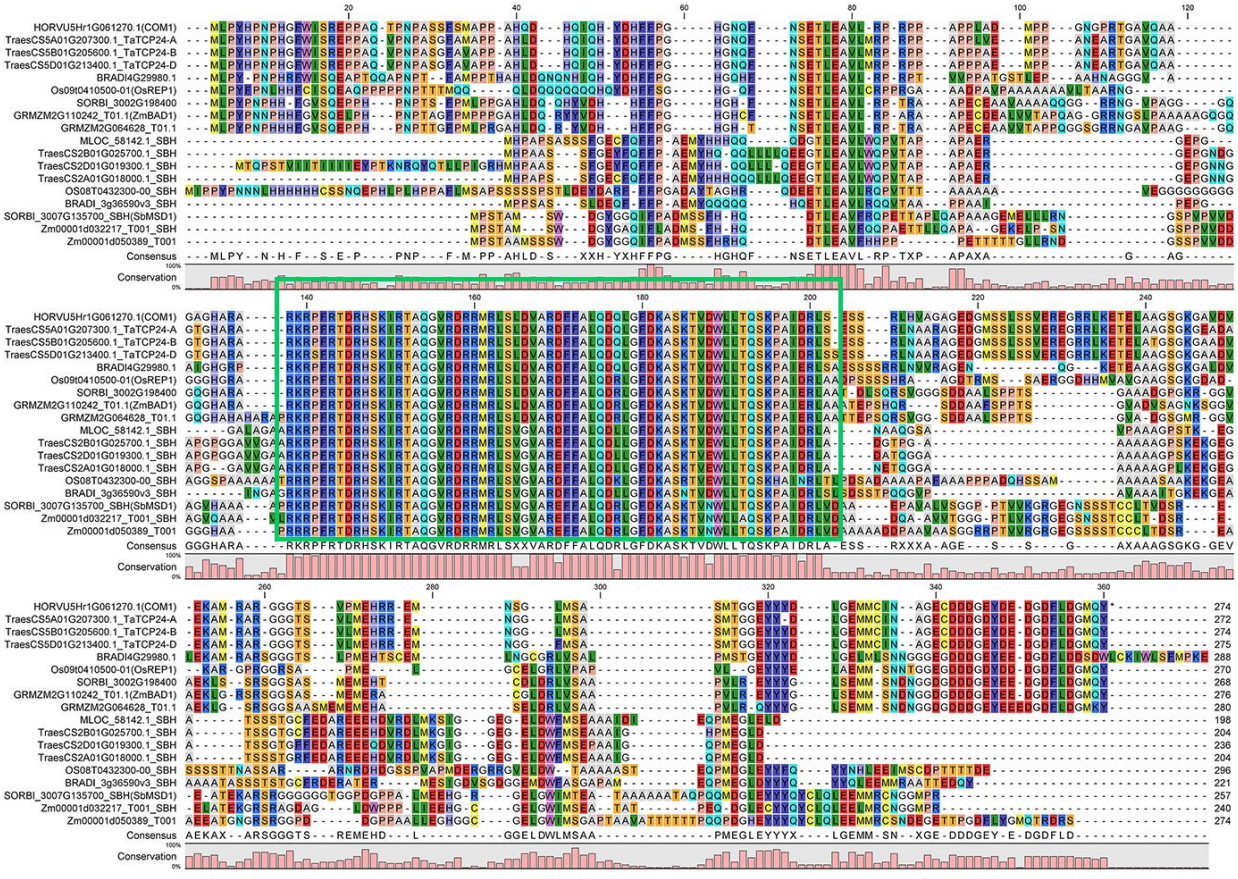

Supplementary Figure 9

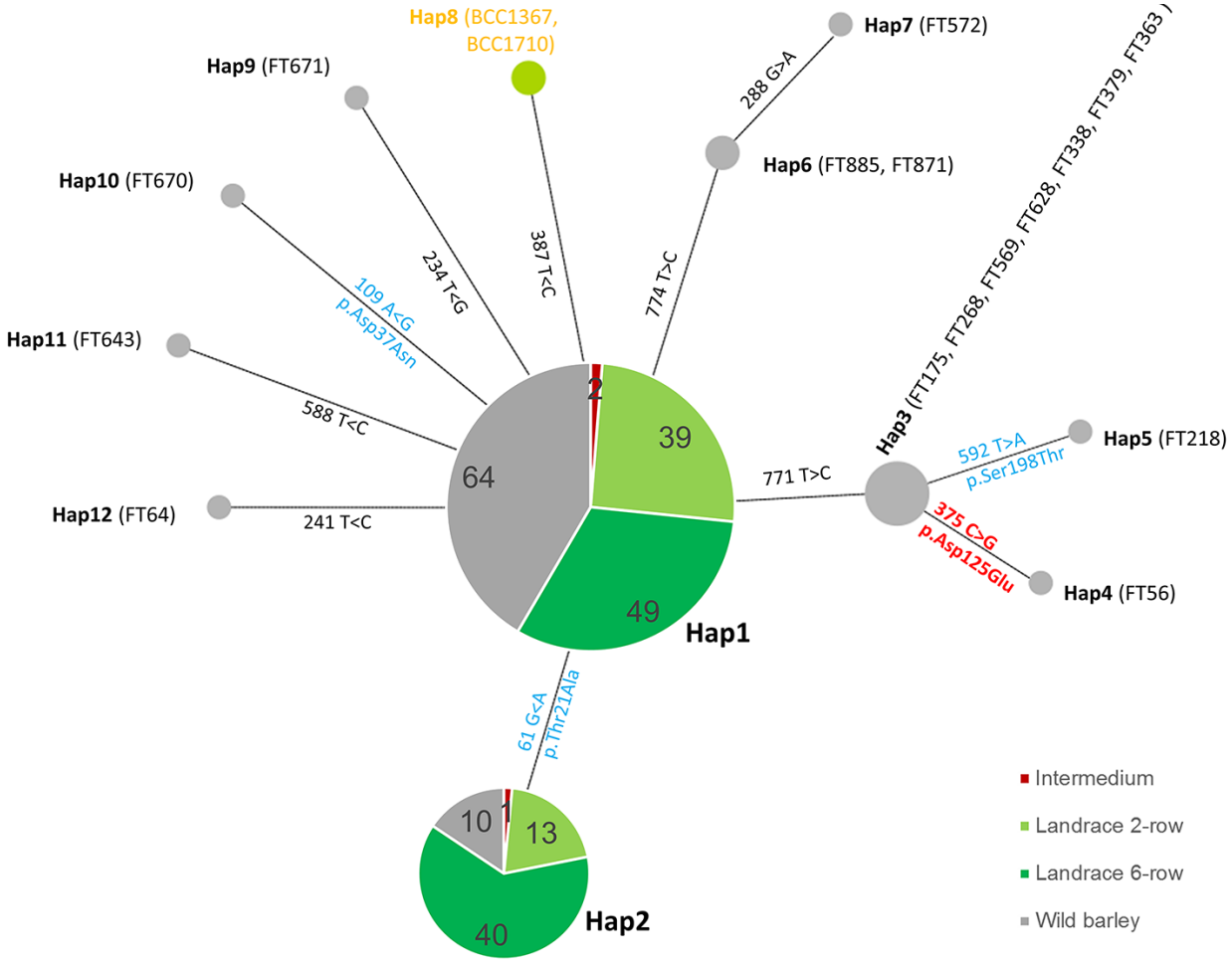

Supplementary Figure 10

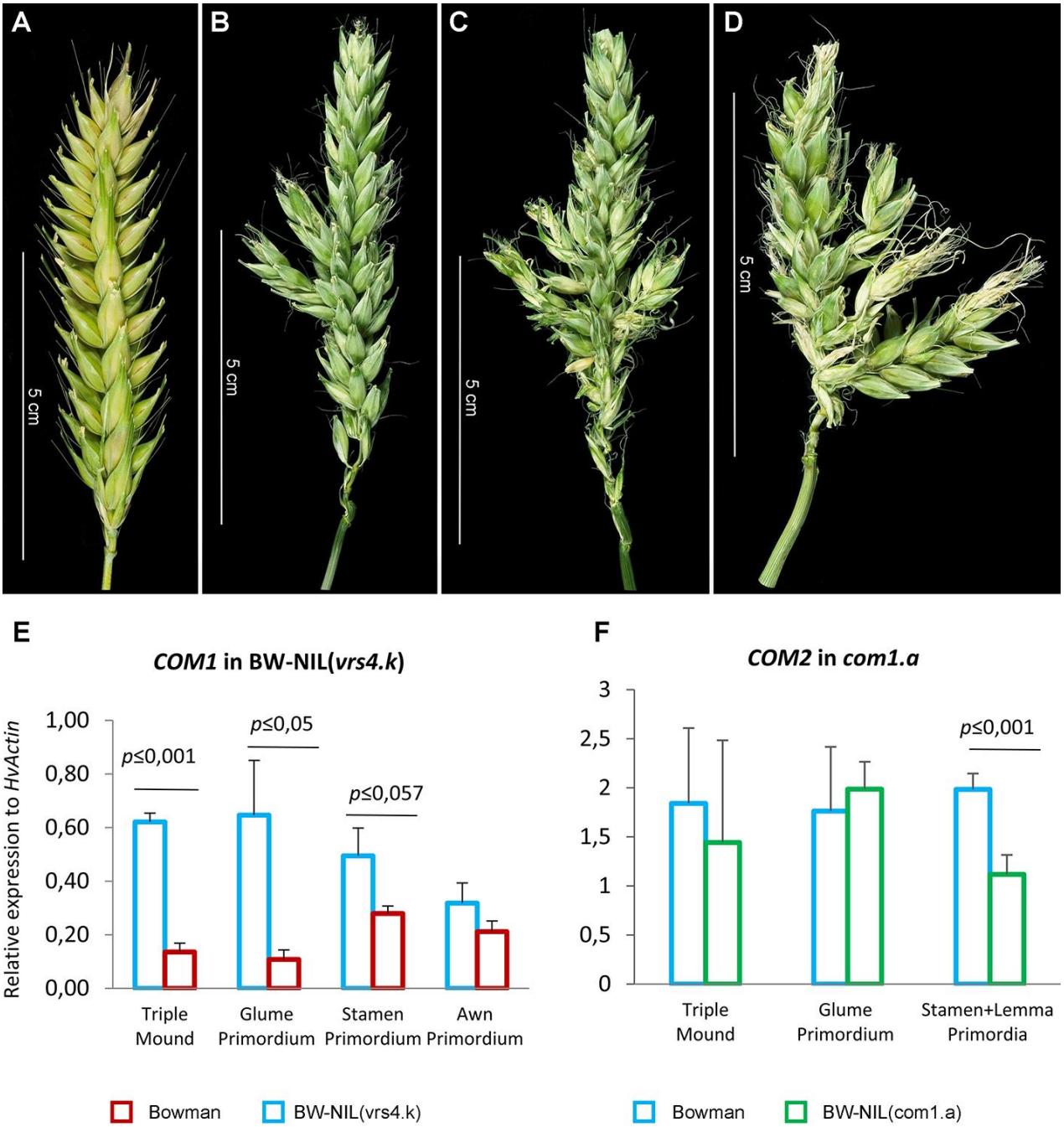

Supplementary Figure 11

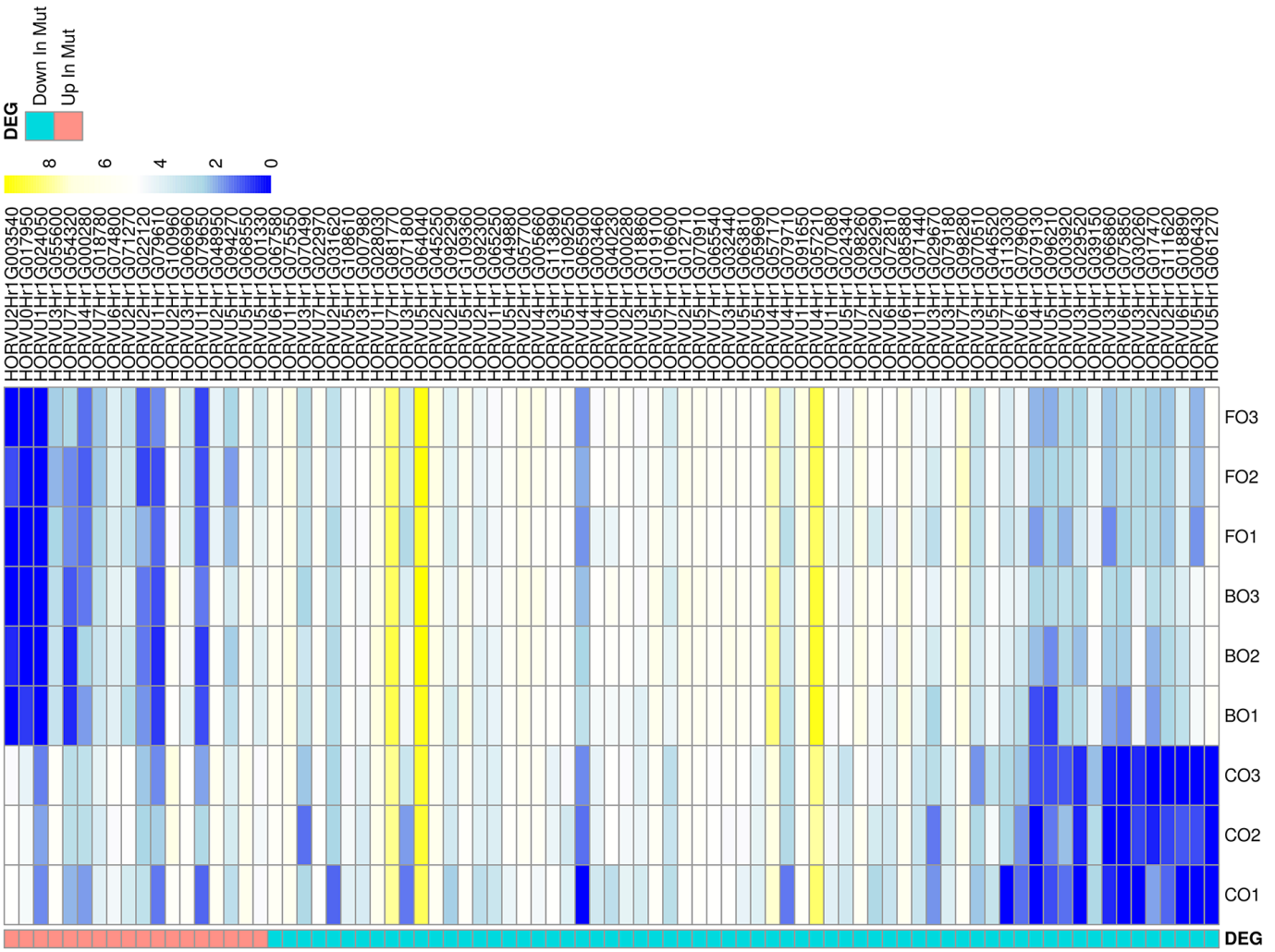

Supplementary Figure 12

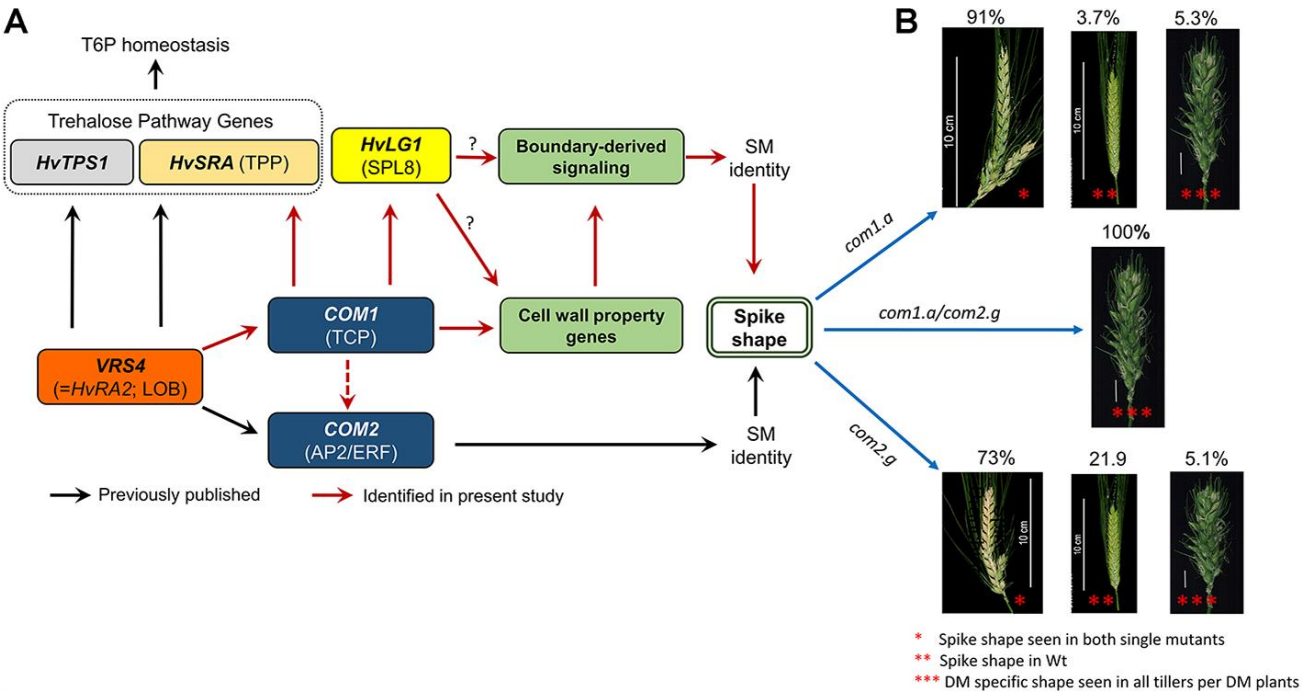

Supplementary tables

Supplementary Table 1. List of the primers

Supplementary Table 2. Graphical genotyping of the critical F_2 recombinants used to develop F_3 families

Supplementary Table 3. Genotypic and phenotypic data of the F_3 progenies

Supplementary Table 4. List of the TILLING as well as induced mutants per corresponding species

Supplementary Table 5. Phenotypic data of the sorghum-TILLING mutants

Supplementary Table 6. Haplotypes identified for *COM1* in barley

Supplementary Table 1. List of the primers							
Primer ID	Species	Application	Marker Type	Orientation	tm	Seq	RE
NGS0015	Barley	genetic mapping	CAPS	FORWARD	60,36	ACTACAGGAGTGCTGCTGGTAAA	SfaNI
NGS0015	Barley	genetic mapping	CAPS	REVERSE	62,07	TTGCGGTATGCAACTCTCAACT	
NGS043	Barley	genetic mapping	CAPS	FORWARD	61,56	TCGAGACTGAGGTAGTGGGACTT	PstI
NGS043	Barley	genetic mapping	CAPS	REVERSE	62,06	CCGAAGGTGGTCAATAGACAAAG	
NGS044	Barley	genetic mapping	CAPS	FORWARD	61,43	GCAACTGGGATTCGATCTCTTAG	EcoRV
NGS044	Barley	genetic mapping	CAPS	REVERSE	61,14	CTAAAGCCTTGCACAAAGTTGG	
NGS045	Barley	genetic mapping	CAPS	FORWARD	62,69	ACACCGAGATGTTGTTGGAAGAG	BtgI
NGS045	Barley	genetic mapping	CAPS	REVERSE	62,07	ATGGATACGGAAGCCAGTGTCTA	
NGS046	Barley	genetic mapping	CAPS	FORWARD	62,15	GATACACTTAAGGCCAAACGGTTC	HinfI
NGS046	Barley	genetic mapping	CAPS	REVERSE	61,58	TACGTCAGCTGGACACACACATA	
NGS048	Barley	genetic mapping	CAPS	FORWARD	62,03	CTCCTACGTGATTCACTGTGTCG	SspI
NGS048	Barley	genetic mapping	CAPS	REVERSE	61,62	TTCAGAGGCTGAAGAAAGAGAGC	
NGS049	Barley	genetic mapping	CAPS	FORWARD	61,95	GGTGATAAATCCACTCCAGCAAC	BbsI
NGS049	Barley	genetic mapping	CAPS	REVERSE	61,82	GTCAAAGTGGAGAAGCTGCAAA	
NGS051	Barley	genetic mapping	CAPS	FORWARD	61,97	TGGTCGTTGGCTTCTCTAGTTTC	PstI

NGS051	Barley	genetic mapping	CAPS	REVERSE	62,17	GAACGAAATCAACACAGGAGACAC	
NGS052	Barley	genetic mapping	CAPS	FORWARD	61,95	GAGAGTAGGCAGATCCAACGAAA	TagI
NGS052	Barley	genetic mapping	CAPS	REVERSE	61,96	CGCGCTCCTAATTATACACAACC	
NGS054	Barley	genetic mapping	CAPS	FORWARD	61,58	TTGGAGTGAGGGTTCTGGTAATC	PstI
NGS054	Barley	genetic mapping	CAPS	REVERSE	61,82	CTCGACTGCTTCGTCCAGTTTA	
NGS084	Barley	genetic mapping	CAPS	FORWARD	62,37	CTTTATTCTCACGTCGTGCACTC	
NGS084	Barley	genetic mapping	CAPS	REVERSE	60,46	TGAAGTAGATGCTCCGTCATCCT	BssHII
NGS094	Barley	genetic mapping	CAPS	FORWARD	61,44	TGCAAGAGCATCTTCCCTTCTT	HhaI
NGS094	Barley	genetic mapping	CAPS	REVERSE	60,28	CTTGCCAACATGCCAAGAGTAG	
NGS158	Barley	genetic mapping	CAPS	FORWARD	61,71	TCAACTACACAAGTTCCCGAATTAAC	BsmAI
NGS158	Barley	genetic mapping	CAPS	REVERSE	62,41	TGTGAGTCATCAAGGTCCAAGG	
NGS160_F	Barley	genetic mapping	CAPS	FORWARD	62,1	GTGGCATCATTAGCATAGGATTACTG	HgaI
NGS160_R	Barley	genetic mapping	CAPS	REVERSE	61,72	AATATGCAAGGTACACCACAAAGAAG	
NGS163	Barley	genetic mapping	CAPS	FORWARD	62,12	CGTATCCGGTGTATCGACGTATT	BsrGI
NGS163	Barley	genetic mapping	CAPS	REVERSE	62,07	TTATCTTCTCTAGAGTGCTGGCTTGA	
NGS164	Barley	genetic mapping	CAPS	FORWARD	63,37	AGCCATGGGCCATTATCTTAATTATC	HhaI
NGS164	Barley	genetic mapping	CAPS	REVERSE	62,83	CATGGAATGCACAACTCCTATGTC	

NGS166	Barley	genetic mapping	CAPS	FORWARD	61,83	AATTCCTGAAACAACGATCAAGTTC	Hpy99I
NGS166	Barley	genetic mapping	CAPS	REVERSE	62,28	CAAGTATGTAATGTTGTGGTGAAGCA	
NGS168	Barley	genetic mapping	CAPS	FORWARD	61,82	CAATATACGCCGTGTCATACTCTCTT	NdeI
NGS168	Barley	genetic mapping	CAPS	REVERSE	62,27	ATATGATCGAGTGGACTGGGAGTT	
NGS169	Barley	genetic mapping	CAPS	FORWARD	62,35	GAGTAGAGGCGCACAGGTGTC	HpyCH41V
NGS169	Barley	genetic mapping	CAPS	REVERSE	61,75	CCAGACATTCTCATTGAAAGAGCTAC	
NGS142_F	Barley	genetic mapping	CAPS	FORWARD		GACGGCCCTGGTATTAGATATG	MboII
NGS142_R	Barley	genetic mapping	CAPS	REVERSE		CCCATCATAACCAAACAGTCCT	
TCP-CDS_F2	Barley	COM1_CDS_resequening	-	FORWARD	61,93	AGGAAGAAGAGAGTCCTCAACCAA	
TCP-CDS_R2	Barley	COM1_CDS_resequening	-	REVERSE	62,88	TAAGCTGCTCGATCGCTAGTACCT	
TCP-CDS_F	Barley	COM1_CDS_resequening	-	FORWARD	63,62	ATATTGTACTCAAGTGCAGGCAGCTACTA	
TCP-CDS_R	Barley	COM1_CDS_resequening	-	REVERSE	62,13	CATGCAATAATTAACTAAGAACATGATGC	
FPC44150-37B_F	Barley	COM1_promotor region	-	FORWARD	61	CACTGTCTATGGAGAGACCACATAGATT	
FPC44150-37B_R	Barley	COM1_promotor region	-	REVERSE	61	GTGAGCTAGGCAGCTAGGTATTTATTAG	
FPC44150-38_F	Barley	COM1_promotor region	-	FORWARD	62,34	TGTTTTCTACTAGTGTCAAGAACCCTACC	
FPC44150-38_R	Barley	COM1_promotor region	-	REVERSE	62,54	GAGAAAATGTGAGTTATCCTGAACCAG	
xNGS129_F	Barley	qPCR	-	FORWARD	60	CGAGCGCATCATGTTCTTAGTTAAT	

xNGS129_R	Barley	qPCR	-	REVERSE	60	AGCAACATAGAACAAAACCATGAGAT	
Com1_ISH_1F20	Barley	In Situ	-	FORWARD		CACAGACGCGAGATGAACAG	
Com1_ISH_1R20	Barley	In Situ	-	REVERSE		AAAAGGCATCACCCTCAAAA	
ActinGene	Barley	qPCR		FORWARD			
ActinGene	Barley	qPCR		REVERSE			
TILLING_Bd-TCP_F1	Brachypodium	Screening of TILLING population	-	FORWARD	57.10	GCAGCAGCAGCAAACTACTA	
TILLING_Bd-TCP_R1	Brachypodium	Screening of TILLING population	-	REVERSE	57.14	GCTTGGACTGAGTGAGCAG	
TILLING_Bd-TCP_F2	Brachypodium	Screening of TILLING population	-	FORWARD	58.48	TTTGACAAGGCCAGCAAG	
TILLING_Bd-TCP_R2	Brachypodium	Screening of TILLING population	-	REVERSE	58.25	AACCACACGCAACAAAGC	
BdACTIN2_F (Bradi1g10630)	Brachypodium	qPCR		FORWARD		GTCGTTGCTCCTCCTGAAAG	
BdACTIN2_R (Bradi1g10630)	Brachypodium	qPCR		REVERSE		ATCCACATCTGCTGGAAGGT	
Bd_TCP_InSitu_F	Brachypodium	qPCR		FORWARD	61.67	CAGACCAAGTTCAGCAGAGATGTAG	
Bd_TCP_InSitu_R	Brachypodium	qPCR		REVERSE	61.72	CCATCCAAATCAAGAGGTGTACTTT	
TILL_SbTCP_F1	Sorghum	Screening of TILLING population		FORWARD	62.25	GAAGAAGCAGTAGCAGTGGCAGTA	
TILL_SbTCP_R1	Sorghum	Screening of TILLING population		REVERSE	62.26	CTTGCTGGCCTTATCGAAGC	
TILL_SbTCP_F2	Sorghum	Screening of TILLING population		FORWARD	62.11	ATGCGGTTGTCCCTCGAC	
TILL_SbTCP_R2	Sorghum	Screening of TILLING population		REVERSE	62.10	GATAGTGAAGAAGTGCTTGCCAGA	

TILL_SbTCP_F3	Sorghum	Screening of TILLING population		FORWARD	62.17	CACTACGTGGACCATCACTTCTTC	
TILL_SbTCP_R3	Sorghum	Screening of TILLING population		REVERSE	62.64	CTAGAGCTCAACTTCTCGGCAACT	
SbActin_F	Sorghum	qPCR		FORWARD		TGGCATCTCTCAGCACATTC	
SbActin_R	Sorghum	qPCR		REVERSE		GGGCGGAAAGAATTAGAAGC	
Sb_TCP_qPCR_F	Sorghum	qPCR		FORWARD	60,07	CACTAGTAGCTAGCTCTTTCTTTATCTGG	
Sb_TCP_qPCR_R	Sorghum	qPCR		REVERSE	60,42	CCAGTAGCATTAACTTAAAGGAGTTCA	
Com2-Bw_SfiI_F	Barley	To screen/sequence for A300C com2 Haplotype in com1.a/com2.g DM population		FORWARD	62.51	CTCCCAGATGATGGCGTTCT	
Com2-Bw_SfiI_R	Barley	To screen/sequence for A300C com2 Haplotype in com1.a/com2.g DM population		REVERSE	62.94	GAACGGCGGGTAGTTGTTGTAG	
iLL_TIL_BdTCP_F1	Brachypodium	illumina sequencing for TILLING mutation detection				TTCCCTACACGACGCTCTTCCGATCTGCAGCAGCAGCAAACTACTA	
iLL_TIL_BdTCP_R1	Brachypodium	illumina sequencing for TILLING mutation detection				AGTTCAGACGTGTGCTCTTCCGATCTGCTTGGACTGAGTGAGCAG	
iLL_TIL_BdTCP_F2	Brachypodium	illumina sequencing for TILLING mutation detection				TTCCCTACACGACGCTCTTCCGATCTTTTGACAAGGCCAGCAAG	
iLL_TIL_BdTCP_R2	Brachypodium	illumina sequencing for TILLING mutation detection				AGTTCAGACGTGTGCTCTTCCGATCTAACCACACGCAACAAAGC	

Supplementary Table 2. Graphical genotyping of the critical F2 recombinants used to develop F3 families															
	Critical F2 recombinants_selected to develop F3														
	1	2	3	4	5	6	7	8	9	10	11	12	13	14	15
Marker ID	4839	5176	5250	5403	5409	5443	5504	4953	5326	5483	5070	5045	174	5407	5488
NGS065	h	h	h	h	h	h	b	b	b	b	a	a	a	a	a
NGS066	h	h	h	h	h	h	b	b	b	b	a	a	a	a	a
NGS046	h	h	h	h	h	h	b	b	b	b	a	a	a	a	a
NGS083	h	h	h	h	h	h	b	b	b	b	a	a	a	a	a
d1652	h	h	h	h	h	h	b	b	b	b	a	a	a	a	a
NGS049	h	h	h	h	h	h	b	b	b	b	a	a	a	a	a
NGS084	h	h	h	h	h	h	b	b	b	b	a	a	a	a	a
NGS168	h	h	h	h	h	h	b	b	b	b	a	a	a	h	a
NGS169	h	b	b	h	h	h	b	b	h	b	h	h	h	h	a
NGS166	h	b	b	h	h	h	b	b	h	b	h	h	h	h	a
com1.a/Phenotype	c	c	c	c	c	c	c	c	c	c	c	c	c	c	a
NGS164	h	b	b	h	h	h	b	b	h	b	h	h	h	h	a
NGS163	h	b	b	h	h	h	b	b	h	b	h	h	h	h	a
NGS160	h	b	b	h	h	h	b	b	h	b	h	h	h	h	a
NGS158	b	b	b	h	h	h	b	h	h	b	h	h	h	h	a
NGS094	b	b	b	b	b	b	h	h	h	h	h	h	h	h	h
NGS111	b	b	b	b	b	b	h	h	h	h	h	h	h	h	h
NGS112	b	b	b	b	b	b	h	h	h	h	h	h	h	h	h
NGS099	b	b	b	b	b	b	h	h	h	h	h	h	h	h	h
NGS142	b	b	b	b	b	b	h	h	h	h	h	h	h	h	h

Supplementary Table 3. Genotypic and phenotypic data of the F3 progenies

CriticalRecF2_ID	GenotypeParentF2_closely linked marker (NGS164 & NGS166)	CriticalRec_ProgenyF3_ID	Genotype_ProgenyF3_NGS169	Phenotype	Number of Spike	Number of Branched Spike
174	h	174 - 1	h	Wt	16	-
174	h	174 - 2	h	Wt	18	-
174	h	174 - 3	h	Wt	17	-
174	h	174 - 4	a	branched	17	13
174	h	174 - 5	b	Wt	20	-
174	h	174 - 6	h	Wt	17	-
174	h	174 - 7	b	Wt	22	-
174	h	174 - 8	b	Wt	21	-
174	h	174 - 9	a	branched	15	12
174	h	174 - 10	a	branched	19	16
174	h	174 - 12	a	branched	14	8
174	h	174 - 13	h	Wt	12	-
174	h	174 - 14	h	Wt	16	-
174	h	174 - 15	h	Wt	14	-
174	h	174 - 16	b	Wt	17	-
4839	h	4839 - 1	h	Wt	15	-
4839	h	4839 - 2	b	Wt	15	-
4839	h	4839 - 3	a	branched	15	6
4839	h	4839 - 4	b	Wt	15	-
4839	h	4839 - 5	a	branched	15	5
4839	h	4839 - 6	b	Wt	13	-
4839	h	4839 - 7	h	Wt	15	-
4839	h	4839 - 8	h	Wt	15	-

4839	h	4839 - 9	a	branched	20	12
4839	h	4839 - 10	b	Wt	14	-
4839	h	4839 - 11	h	Wt	16	-
4839	h	4839 - 12	h	Wt	19	-
4839	h	4839 - 13	h	Wt	20	-
4839	h	4839 - 14	h	Wt	19	-
4839	h	4839 - 15	h	Wt	19	-
4839	h	4839 - 16	h	Wt	12	-
4953	b	4953 - 1	b	Wt	13	-
4953	b	4953 - 2	b	Wt	15	-
4953	b	4953 - 3	b	Wt	14	-
4953	b	4953 - 4	b	Wt	13	-
4953	b	4953 - 5	b	Wt	16	-
4953	b	4953 - 6	b	Wt	17	-
4953	b	4953 - 7	b	Wt	13	-
4953	b	4953 - 8	b	Wt	18	-
4953	b	4953 - 9	b	Wt	13	-
4953	b	4953 - 10	b	Wt	15	-
4953	b	4953 - 11	b	Wt	19	-
4953	b	4953 - 12	b	Wt	16	-
4953	b	4953 - 13	b	Wt	19	-
4953	b	4953 - 14	b	Wt	14	-
4953	b	4953 - 15	b	Wt	15	-
4953	b	4953 - 16	b	Wt	17	-
5045	h	5045 - 1	a	branched	19	10
5045	h	5045 - 2	h	Wt	14	-
5045	h	5045 - 3	h	Wt	11	-
5045	h	5045 - 5	h	Wt	14	-
5045	h	5045 - 6	h	Wt	16	-

5045	h	5045 - 7	h	Wt	20	-
5045	h	5045 - 8	a	branched	15	6
5045	h	5045 - 9	h	Wt	15	-
5045	h	5045 - 10	h	Wt	18	-
5045	h	5045 - 11	a	branched	12	5
5045	h	5045 - 13	h	Wt	20	-
5045	h	5045 - 14	h	Wt	19	-
5045	h	5045 - 15	h	Wt	15	-
5045	h	5045 - 16	h	Wt	15	-
5070	h	5070 - 1	h	Wt	16	-
5070	h	5070 - 2	h	Wt	17	-
5070	h	5070 - 3	h	Wt	15	-
5070	h	5070 - 4	a	branched	16	11
5070	h	5070 - 5	b	Wt	20	-
5070	h	5070 - 6	h	Wt	21	-
5070	h	5070 - 7	a	branched	17	9
5070	h	5070 - 8	a	branched	16	8
5070	h	5070 - 9	b	Wt	18	-
5070	h	5070 - 11	b	Wt	25	-
5070	h	5070 - 12	a	branched	14	9
5070	h	5070 - 13	h	Wt	15	-
5070	h	5070 - 14	h	Wt	14	-
5070	h	5070 - 15	h	Wt	26	-
5070	h	5070 - 16	a	branched	19	11
5176	b	5176 - 1	b	Wt	13	-
5176	b	5176 - 2	b	Wt	16	-
5176	b	5176 - 3	b	Wt	21	-
5176	b	5176 - 4	b	Wt	13	-
5176	b	5176 - 5	b	Wt	14	-

5176	b	5176 - 6	b	Wt	16	-
5176	b	5176 - 7	b	Wt	28	-
5176	b	5176 - 8	b	Wt	12	-
5176	b	5176 - 9	b	Wt	14	-
5176	b	5176 - 10	b	Wt	25	-
5176	b	5176 - 11	b	Wt	16	-
5176	b	5176 - 12	b	Wt	12	-
5176	b	5176 - 13	b	Wt	13	-
5176	b	5176 - 14	b	Wt	13	-
5176	b	5176 - 15	b	Wt	19	-
5176	b	5176 - 16	b	Wt	16	-
5250	b	5250 - 1	b	Wt	13	-
5250	b	5250 - 2	b	Wt	13	-
5250	b	5250 - 3	b	Wt	18	-
5250	b	5250 - 4	b	Wt	16	-
5250	b	5250 - 5	b	Wt	13	-
5250	b	5250 - 6	b	Wt	12	-
5250	b	5250 - 7	b	Wt	14	-
5250	b	5250 - 8	b	Wt	17	-
5250	b	5250 - 9	b	Wt	16	-
5250	b	5250 - 10	b	Wt	13	-
5250	b	5250 - 11	b	Wt	13	-
5250	b	5250 - 12	b	Wt	15	-
5250	b	5250 - 13	b	Wt	21	-
5250	b	5250 - 14	b	Wt	18	-
5250	b	5250 - 15	b	Wt	15	-
5250	b	5250 - 16	b	Wt	16	-
5326	h	5326 - 1	h	Wt	16	-
5326	h	5326 - 2	b	Wt	17	-

5326	h	5326 - 3	h	Wt	15	-
5326	h	5326 - 4	h	Wt	15	-
5326	h	5326 - 5	b	Wt	13	-
5326	h	5326 - 6	b	Wt	16	-
5326	h	5326 - 7	h	Wt	17	-
5326	h	5326 - 8	h	Wt	16	-
5326	h	5326 - 9	a	branched	16	8
5326	h	5326 - 10	b	Wt	11	-
5326	h	5326 - 11	b	Wt	15	-
5326	h	5326 - 12	h	Wt	16	-
5326	h	5326 - 13	a	branched	13	10
5326	h	5326 - 14	b	Wt	12	-
5326	h	5326 - 15	b	Wt	11	-
5326	h	5326 - 16	h	Wt	15	-
5403	h	5403 - 1	h	Wt	15	-
5403	h	5403 - 2	h	Wt	16	-
5403	h	5403 - 3	a	branched	17	13
5403	h	5403 - 4	h	Wt	13	-
5403	h	5403 - 5	b	Wt	17	-
5403	h	5403 - 6	a	branched	14	9
5403	h	5403 - 7	a	branched	16	10
5403	h	5403 - 8	h	Wt	15	-
5403	h	5403 - 9	h	Wt	13	-
5403	h	5403 - 10	b	Wt	16	-
5403	h	5403 - 12	b	Wt	18	-
5403	h	5403 - 13	h	Wt	15	-
5403	h	5403 - 14	b	Wt	15	-
5403	h	5403 - 15	a	branched	15	9
5403	h	5403 - 16	b	Wt	16	-

5407	h	5407 - 1	a	branched	15	8
5407	h	5407 - 2	h	Wt	19	-
5407	h	5407 - 3	b	Wt	13	-
5407	h	5407 - 4	h	Wt	14	-
5407	h	5407 - 5	h	Wt	14	-
5407	h	5407 - 6	a	branched	15	11
5407	h	5407 - 7	h	Wt	14	-
5407	h	5407 - 8	h	Wt	15	-
5407	h	5407 - 9	h	Wt	15	-
5407	h	5407 - 10	b	Wt	13	-
5407	h	5407 - 11	h	Wt	16	-
5407	h	5407 - 12	a	branched	18	10
5407	h	5407 - 13	a	branched	16	12
5407	h	5407 - 14	h	Wt	15	-
5407	h	5407 - 15	h	Wt	14	-
5407	h	5407 - 16	h	Wt	15	-
5409	h	5409 - 1	-	Wt	16	-
5409	h	5409 - 2	h	Wt	13	-
5409	h	5409 - 3	h	Wt	13	-
5409	h	5409 - 4	b	Wt	13	-
5409	h	5409 - 5	h	Wt	14	-
5409	h	5409 - 6	a	branched	15	11
5409	h	5409 - 7	a	branched	19	7
5409	h	5409 - 8	h	Wt	13	-
5409	h	5409 - 9	h	Wt	16	-
5409	h	5409 - 11	h	Wt	19	-
5409	h	5409 - 13	h	Wt	13	-
5409	h	5409 - 14	a	branched	16	11
5409	h	5409 - 15	b	Wt	13	-

5409	h	5409 - 16	b	Wt	14	-
5443	h	5443 - 1	h	Wt	14	-
5443	h	5443 - 2	a	branched	12	7
5443	h	5443 - 3	h	Wt	14	-
5443	h	5443 - 4	b	Wt	13	-
5443	h	5443 - 5	h	Wt	13	-
5443	h	5443 - 6	h	Wt	18	-
5443	h	5443 - 7	a	branched	17	10
5443	h	5443 - 8	a	branched	12	9
5443	h	5443 - 9	b	Wt	14	-
5443	h	5443 - 11	h	Wt	12	-
5443	h	5443 - 12	h	Wt	14	-
5443	h	5443 - 13	h	Wt	14	-
5443	h	5443 - 14	a	branched	16	12
5443	h	5443 - 15	a	branched	14	10
5443	h	5443 - 16	b	Wt	15	-
5483	b	5483 - 1	b	Wt	15	-
5483	b	5483 - 2	b	Wt	15	-
5483	b	5483 - 3	b	Wt	15	-
5483	b	5483 - 4	b	Wt	13	-
5483	b	5483 - 5	b	Wt	11	-
5483	b	5483 - 6	b	Wt	13	-
5483	b	5483 - 7	b	Wt	16	-
5483	b	5483 - 8	b	Wt	14	-
5483	b	5483 - 9	b	Wt	15	-
5483	b	5483 - 10	b	Wt	14	-
5483	b	5483 - 11	b	Wt	14	-
5483	b	5483 - 12	b	Wt	16	-
5483	b	5483 - 13	b	Wt	12	-

5483	b	5483 - 14	b	Wt	14	-
5483	b	5483 - 15	b	Wt	15	-
5483	b	5483 - 16	b	Wt	13	-
5488	a	5488 - 2	a	branched	22	15
5488	a	5488 - 3	a	branched	23	14
5488	a	5488 - 5	a	branched	19	14
5488	a	5488 - 6	a	branched	12	10
5488	a	5488 - 7	a	branched	21	15
5488	a	5488 - 8	a	branched	17	13
5488	a	5488 - 9	a	branched	20	11
5488	a	5488 - 10	a	branched	20	10
5488	a	5488 - 11	a	branched	23	13
5488	a	5488 - 12	a	branched	25	16
5488	a	5488 - 13	a	branched	20	14
5488	a	5488 - 14	a	branched	20	12
5488	a	5488 - 15	a	branched	21	12
5488	a	5488 - 16	a	branched	20	10
5504	b	5504 - 1	b	Wt	15	-
5504	b	5504 - 2	b	Wt	19	-
5504	b	5504 - 3	b	Wt	24	-
5504	b	5504 - 4	b	Wt	21	-
5504	b	5504 - 5	b	Wt	21	-
5504	b	5504 - 6	b	Wt	17	-
5504	b	5504 - 7	b	Wt	19	-
5504	b	5504 - 8	b	Wt	11	-

Supplementary Table 4. Part 1. List of the TILLING as well as induced mutants per corresponding species

Species	TILLING Line ID	DNA Position (from Start Codon)	SNP type	Homo/ Hetero	Wild aa	Mutant aa	Location within the gene	the grass sp. with deviated aa	SIFT prediction	SIFT score
Barley	M3.15104	305	G-to-A	homo	R	K	within TCP Domain	no change in grass; R	NA	NA
Barley	M3.4406	334	G-to-A	homo	A	T	within TCP Domain	no change in grass; A	NA	NA
Barley	M3.2598	346	C-to-T	homo	R	W	within TCP Domain	no change in grass; R	NA	NA
Barley	M3.13729	335	C-to-T	homo	A	V	within TCP Domain	no change in grass; A	NA	NA
Barley	M3.4063	211	C-to-T	hetro	P	S	befor TCP Domain	OS: D	NA	NA
Barley	M3.9299	595	G-to-A	hetro	G	R	after TCP Domain	no change in grass; G	NA	NA
Barley	M3.14287	109	G-to-A	hetro	D	N	befor TCP Domain	OS: Q	NA	NA
Barley	M3.2821	241	C-to-T	hetro	p	S	befor TCP Domain	in OS, Tu, BD and SB: A	NA	NA
Barley	M3.14325	242	C-to-A	hetro	p	Q	befor TCP Domain	in OS, Tu, BD and SB: A	NA	NA
Barley	M3.6995	290	G-to-A	homo	R	K	befor TCP Domain	no change in grass; R	NA	NA
Barley	M3.12123	290	G-to-A	hetro	R	K	befor TCP Domain	no change in grass; R	NA	NA
Barley	M3.13483	290	G-to-A	hetro	R	K	befor TCP Domain	no change in grass; R	NA	NA
Barley	M3.2927	496	C-to-T	homo	L	F	after TCP Domain	OS: S, ZM: E, Sb: L	NA	NA
Barley	M3.13996	511	G-to-A	hetro	A	T	after TCP Domain	ZM: R, Sb: V	NA	NA
Barley	M3.14152	514	G-to-A	homo	G	R	after TCP Domain	OS: A, ZM: -	NA	NA
Barley	M3.6504	515	G-to-A	hetro	G	E	after TCP Domain	OS: A, ZM: -	NA	NA
Barley	M3.3717	528	G-to-A	hetro	M	I	after TCP Domain	in OS: R, BD: -, SB: - , ZM: -	NA	NA
Barley	M3.11298	544	G-to-A	hetro	V	M	after TCP Domain	in OS: A, BD: -, SB: D , ZM: D	NA	NA
Barley	M3.11933	544	G-to-A	homo	V	M	after TCP Domain	in OS: A, BD: -, SB: D , ZM: D	NA	NA
Barley	M3.13403	544	G-to-A	hetro	V	M	after TCP Domain	in OS: A, BD: -, SB: D , ZM: D	NA	NA
Barley	M3.6448	573	G-to-T	hetro	E	D	after TCP Domain	in OS: V, SB: S , ZM: S	NA	NA
Barley	M3.12394	595	G-to-A	hetro	G	R	after TCP Domain	no change in grass; G	NA	NA

Barley	M3.3609	635	G-to-A	homo	R	k	after TCP Domain	no change in grass; R	NA	NA
Barley	M3.9852	641	G-to-A	hetro	G	D	after TCP Domain	no change in grass; G	NA	NA
Barley	M3.11856	670	C-to-T	homo	R	C	after TCP Domain	in OS: -, BD: L, SB: - , ZM: -	NA	NA
Sorghum	ARS152	188	G-to-A	hetro	R	H	Befor TCP Domain	not conserved	NA	NA
Sorghum	ARS180	430	A-to-G	homo	A	T	within TCP Domain	no change in grass; A	NA	NA
Sorghum	ARS137	577	C-to-T	hetro	P	S	after TCP Domain	not conserved	NA	NA
Brachypodium	8004	173	C_To_T		S58F		Befor TCP Domain		Damaging	0
Brachypodium	8231	187	G_To_A		A63T		Befor TCP Domain		Damaging	0
Brachypodium	8566	266	G_To_A		G89D		Befor TCP Domain		Damaging	0,01
Brachypodium	7576	278	C_To_T		A93V		Befor TCP Domain		Damaging	0,01
Brachypodium	4957	295	C_To_T		P99S		Befor TCP Domain		Damaging	0,05
Brachypodium	5446	346	C_To_T		Q116*		within TCP Domain		-	-
Brachypodium	8373	437	G_To_A		S146N		within TCP Domain		Damaging	0,02
Brachypodium	5149	472	C_To_T		P158S		within TCP Domain		Tolerated	0,07
Brachypodium	5337	533	C_To_T		A178V		within TCP Domain		Tolerated	0,15
Brachypodium	6339	536	G_To_A		G179E		within TCP Domain		Tolerated	0,07
Brachypodium	4196	785	G_To_A		G262D		after TCP Domain		Damaging	0

Supplementary Table 4. Part 2.								
Running Number	Branched (compositum) Barleys:	Gene Bank	Type	ID	type of mutation and the doner line	Cross with com1a	PCR with TCP_potential promotor based primers	TCP _CDS_Resequening
4	Mut.3906	GER	Spring	MHOR347	X-ray; spike with short branches; 1949- 'Heines Haisa';	Done/allelic	Amplicon observed	No Amplicon
8	com1.j	USA	Spring	NGB2020	X-ray; induced mutant in Donaria (PI 161974) isolated by F. Scholz		No Amplicon	No Amplicon
int-h 42	int-h 42	SWE	#N/A	#N/A	/neutrons/ KRISTINA		No Amplicon	No Amplicon
int-h 43	int-h 43	SWE	#N/A	#N/A	/hydroxy n-propyl methanesulfonate/ KRISTINA		No Amplicon	No Amplicon
int-h 44	int-h 44	SWE	#N/A	#N/A	/ethyl methanesulfonate/ KRISTINA		No Amplicon	No Amplicon

Supplementary Table 5. Phenotypic data of the sorghum-TILLING mutants

			M5 generation _to measure branch number			M6 generation _to measure branch angle				
TILLING Line ID_M4	DNA Position (from Start Codon)	Location within the gene	Number of plants _all homozygous	Average No of nodes/panicle/ family	Average No of branch per nodes/panicle/ family	Number of plants _ all homozygous	No of nodes/panicle/family	Average No of angle per nodes/panicle/ family	Average angle size (degree) per nodes/panicle/ family	Grain formation
ARS180	A430G	within TCP Domain	8	12	4,2*	7	3 basal	10,1	5,2***	only 20-40 grains/panicle
ARS137	C577T	after TCP Domain	8	11,5	4,4*	6	3 basal	9,3	15,9	Complete fertility
Wt BT623	-	-	7	10	5,4	5	3 basal	8,1	10,95	Complete fertility

* ; ttest ($P < 0.05$)
*** ; ttest ($P < 0.001$)

1225 **Supplementary source data**

1226 **Supplementary source data 1. Differentially expressed genes in Wt and barley mutant with**

1227 **the corresponding statistical values**

1228